ROBUST RESOURCE ADEQUACY PLANNING IN THE FACE OF COAL RETIREMENTS

Roger Lueken[†,§*], Jay Apt [‡,§], Fallaw Sowell[‡]

† Present address: The Brattle Group, 1850 M Street NW, Suite 1200, Washington D.C. 20036, USA
§ Department of Engineering and Public Policy, Carnegie Mellon University, Pittsburgh, PA 15213, USA
‡ Tepper School of Business, Carnegie Mellon University, Pittsburgh, PA 15213, USA
*Corresponding Author. E-mail: Roger.Lueken@brattle.com. Telephone: 202-419-3321.

Abstract

Over the next decade, many U.S. coal-fired power plants are expected to retire, posing a challenge to system planners. We investigate the resource adequacy requirements of the PJM Interconnection, and how procuring less capacity may affect reliability. Assuming that plant forced outages are independent of one another, we find that PJM's 2010 reserve margin of 20.5% was sufficient to achieve the stated reliability standard of one loss of load event per ten years with 90% confidence. PJM could reduce reserve margins to 13% and still achieve levels of reliability accepted by other U.S. and international power systems with 90% confidence. Reducing reserve margins from 20.5% to 13% would reduce PJM's capacity procurement by 11 GW, the same amount of coal capacity that PJM has identified as at high risk of retirement. However, if plant failures are caused by external events such as extreme weather and are correlated, reliability may be significantly lower than forecast by PJM's current resource planning process (we consider correlated outages in sections 1.2.4 and 1.3.6). The risk posed by supply shortages is primarily due to very rare, but severe events. System operators should work to ensure that the system is robust to these extreme events.

1.1 Introduction

Over the next decade, significant coal plant retirements are expected in the United States. The Energy Information Agency forecasts that 40 GW of coal capacity will retire between 2014 – 2020 (EIA 2013). These retirements are due to a combination of factors. Many coal plants are near the end of their expected lifespan. Many small and outdated coal plants are finding it cost prohibitive to make the retrofits necessary to comply with emission regulations. Low natural gas prices have put downward pressure on revenues from wholesale electricity prices.

These retirements pose a new challenge to system operators, who are mandated to meet resource adequacy requirements. To meet these requirements, systems procure generation capacity that is rarely used but is needed in extreme circumstances. This capacity, typically natural gas combustion turbines, has low upfront capital costs but high operating costs. In the traditional regulated utility model, these generators are compensated through rate-of-return ratemaking, even if they produce no power. The restructuring of 20 U.S. states in the late 1990s and early 2000s led to the industry to recognize the so-called "missing money problem", whereby market designs would not support sufficient generation investment (Spees et al 2013). Today, most restructured markets use capacity markets to compensate generators for the capacity they provide.

In both traditional regulated utilities and systems with capacity markets, the system operator centrally models the amount of capacity needed to achieve a given resource adequacy standard. These models consider the reliability of existing generators and forecasts of load. Both generator outages and load forecasts are highly uncertain, creating the risk that inaccurate modeling may lead to an over- or under-procurement of capacity. Over-procuring capacity will increase costs for ratepayers; under-procuring capacity will create outage risks above reliability targets.

The traditional metric of resource adequacy is the number of loss of load events (LOLE) per ten years. Most U.S. systems, including the PJM Interconnection, procure enough capacity to meet a LOLE standard of one expected event per ten years, or 0.1 events per year (0.1 LOLE standard) (PJM 2013). The 0.1 LOLE standard dates back to the 1950s, although its origins are unknown (EISPC 2013). Here we follow the standard definition of an outage "event" as an outage lasting one or more consecutive hours. The LOLE metric is problematic, in that it does not consider either the duration of an outage, or magnitude of load that is shed during an outage.

Due to the limitations of the LOLE metric, some systems have adopted other standards. The Southwest Power Pool (SPP) uses the metric of 24 expected loss of load hours (LOLH) per ten years, or 2.4 hours per year (2.4 LOLH standard) (EISPC 2013). The Scandinavian system uses the metric of expected unserved energy (UE) totaling 0.001% of total load served (0.001% UE standard). Australia's National Energy Market (NEM) and South West Interconnected System (SWIS) have adopted a 0.002% UE standard (Pfeifenberger et al 2013). The North American Electric Reliability Corporation has recommended system operators adopt UE standards, as they explicitly consider the magnitude of outages (NERC 2010). All three metrics consider only the risk of generator outages, and exclude other risks such as transmission or distributions outages.

Resource planners base their capacity procurement decisions on the expected value of the metric used (0.1 LOLE, 2.4 LOLH, 0.001% UE). By considering only the expected value, resource planners imply that they are risk neutral to supply shortages. However, evidence suggests system operators are highly risk averse to supply shortages, as these shortages reflect poorly on the system operator, draw unwanted public attention, and can cause a host of grid management problems such as network collapse, leading to cascading failures (Joskow and Tirole 2007).

Although a significant body of literature exists on the electric system reliability, resource adequacy risks have received less attention. As part of a study into electricity reliability more broadly, (Hines et al 2009) find that supply shortages over the period 1984 – 2006 were responsible only for 2.3% of U.S. outage events. The methods used by system planners today are very similar to those outlined by Billinton in the 1970s (Billinton et al 1973). More recently, system planners have begun to analyze the economically optimal reserve margin, or the reserve margin that minimizes total system costs and outage costs (Pfeifenberger et al 2013).

Here we analyze the resource adequacy requirements of the PJM Interconnection, and how future retirements could affect reliability. PJM anticipates 11 GW of coal capacity, or ~7% of total capacity, is "at high risk" of retirement (PJM 2011b). Since 2007, PJM has procured capacity through its centralized capacity market. Capacity market billings were $8 billion in both the 2009/2010 and 2010/2011 auctions. In 2010, capacity costs were roughly 18% of total 2010 billings (PJM 2011a).

PJM uses a forecasting model to calculate the capacity needed to meet the 0.1 LOLE standard (PJM 2003). The robustness of this model is important, as it sets the amount of capacity PJM procures, and therefore costs on the capacity and energy markets. However, it is difficult to verify the model's accuracy due to the rarity of supply shortages in PJM.

We develop a robust statistical model of resource adequacy in PJM for the year 2010. The model consists of a probabilistic forecast of hourly load and a probabilistic forecast of generator outages. The load model explicitly considers three major drivers of uncertainty: uncertain load growth, natural temperature variability, and uncertainty in the underlying model/process. The load model uses five years of load data and sixty years of temperature data from Pittsburgh International

Airport and Reagan National Airport. We combine the load and outage models into a probabilistic forecast of supply shortages.

We analyze the sensitivity of LOLE, LOLH, and UE to PJM's reserve margin, measured in terms of installed capacity. In 2010, PJM calculated a 15.5% reserve margin was needed to achieve the 0.1 LOLE standard. PJM procured more capacity than needed, making the realized reserve margin 20.5%. We vary PJM's reserve margin from 10% - 25% to see how LOLE, LOLH, and UE change.

We find that PJM's 15.5% reserve margin target met the 0.1 LOLE standard. By procuring additional capacity such that the actual reserve margin was 20.5%, PJM's revealed risk preference was to meet the 0.1 LOLE standard with 90% confidence.

PJM could reduce reserve margins to 13% or 14% by switching to the 2.4 LOLH or 0.001% UE standard, while maintaining current risk preferences. This represents a 9 – 11 GW reduction in capacity from a 20.5% reserve margin. We therefore conclude that PJM could significantly reduce reserve margins and still maintain reliability standards commonly used by other systems and current risk preferences. More specifically, the 11 GW of coal capacity identified by PJM as "at high risk" of retirement could retire.

However, the risk of a supply shortage rises if the potential for correlated outages among generators is considered. We show that the risk of a natural gas supply disruption to PJM's natural gas combustion turbines could increase outage risk, and cause PJM to underestimate this risk.

We also find that the distribution of outage size is 'fat tailed', and the largest 10% of outages account for half of total load shed. Therefore, system operators should recognize that supply shortages are more rare, but more disruptive than implied by reliability metrics.

1.2 Methods

We develop a probabilistic forecast of supply shortages in PJM for 2010. This forecast consists of two separate analyses: a probabilistic simulation of hourly load, and a probabilistic simulation of capacity available at each hour. These analyses are described in detail below. We then use Monte Carlo analysis to find the probability that load exceeds supply for each hour of the year. We analyze three reliability metrics: LOLE, LOLH, and UE, and their sensitivity to PJM's reserve margin. We perform several sensitivity analyses, and compare the results of our simulation to PJM's modeling of capacity needs.

1.2.1 Load forecast

We use historic load and temperature data to forecast load in PJM. Load forecasts have three sources of uncertainty: uncertainty in load growth, natural temperature variability, and uncertainty in the underlying model/process. We consider each separately to robustly forecast load.

A large literature exists on forecasting load. Techniques commonly used include regression analysis, time-series analysis, and neural networks (PJM 2013, Hagan and Behr 1987, Hippert et al 2001). The model used by PJM to set reserve margin targets is a probabilistic model derived from Billinton (PJM 2003, Billinton et al 1973). The model is not regression based, but uses heuristics that PJM has developed over time. PJM uses a separate regression model to forecast long-term load growth (PJM 2013).

We use regression analysis to forecast hourly load in PJM. The regression model shares many features in common with the regression model PJM uses to forecast long-term load growth. Regression analysis is useful for estimating the expected value of load at each time period. However, our focus is extreme events, i.e. high-load hours in which outages are more likely. To account for

these extreme events, we bootstrap the model's residuals to simulate uncertainty in load at each time period.

We forecast hourly load in 2010 using hourly data from the previous five years. Using five years worth of data results in higher accuracy than if 10 or 15 years of data were considered. This is because the relationship between temperature and load has changed in PJM over time, with loads becoming increasingly sensitive to high temperatures. Using data more than five years old causes the model to under-forecast load at high temperatures. For more details, see Appendix A.

Hourly load data is from PJM (PJM 2014a). Hourly temperature and associated weather data is from the National Oceanic and Atmospheric Association (NOAA) for the Reagan National Airport and Pittsburgh International Airport weather stations (NOAA 2014a). These weather stations were chosen as they have reliable temperature data available dating back to the 1940s, which is used to forecast 2010 temperatures. Data on the minutes of daylight for each day is from (US Naval Observatory, 2012) for Washington DC.

Since its inception, the PJM territory has undergone several expansions (Table 1). To account for these expansions, we forecast load separately for "PJM Classic" (the PJM region prior to any expansions) and each expansion zone. We then combine the forecasts into an overall PJM load forecast.

Table 1. PJM Expansions, 1993 – 2010 (PJM 2014a)

Expansion	Date
Rockland Energy	March 2002
Allegheny Energy	April 2002
Exelon – Commonwealth Edison	May 2004
AEP	October 2004
Dayton Power & Light	October 2004
Duquesne Light Co	January 2005
Dominion Virginia	May 2005

For each zone, the analysis has the following seven steps:

Step 1: Regress long-term trend

We first identify and remove the five year, long-term trend in load growth. By removing the long-term trend, we are able to explicitly incorporate PJM's forecast of future load growth (step 5). To remove the long-term trend, we use a non-parametric, additive model and regress load against the hour index, as shown in Eq. (1)[1]. The hour index starts at 1 for the first hour of 2005, and ends at the last hour of 2009. Using an additive model allows us to account for nonlinearities in load growth, and regressing the logarithm of load allows us to account for higher variability at high-load hours. The model's residuals, β_0, are stationary. We use these residuals in step 2. Figure 1 shows the long-term trend of "PJM Classic", the original PJM footprint, and the model's stationary residuals.

$$\log(load) = \beta_0 + \beta_1 hourIndex \quad (1)$$

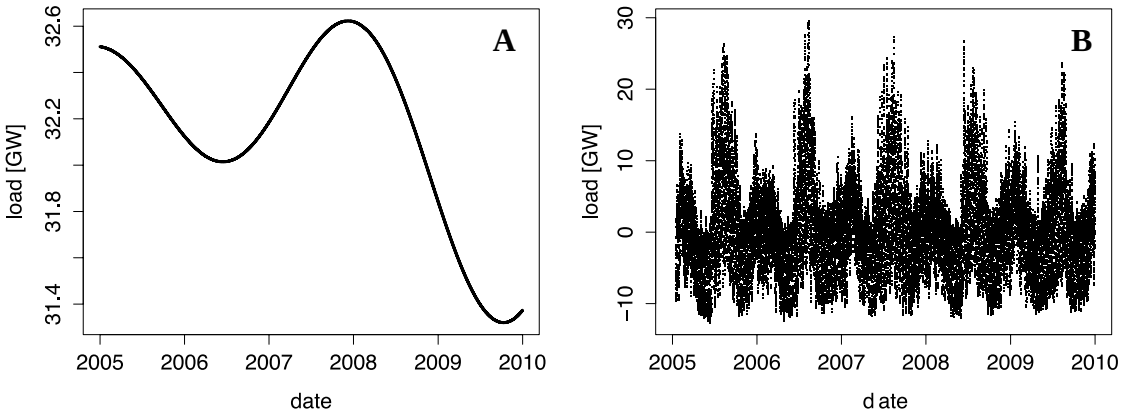

[1] Non-parametric, additive terms calculated using R software and *gam* command from 'gam' package in R with default settings, see (Hastie, 2013).

Figure 1. (A) Fitted long-term trend and (B) stationary hourly residuals, β_0, for PJM Classic.

Step 2: Regress stationary time series

The second step is to regress β_0, the stationary residuals from step 1, on several explanatory variables, including calendar events such as major holidays and weekends, temperature, and length of daylight hours. This is shown in Eq. (2). For hour of the day and length of daylight hours, we include interaction terms with the month of the year to account for changes in electric load patterns throughout the year. Table A.1 lists all explanatory variables. We use model's residuals, γ_0, to account for uncertainty in the underlying model/process (see step 7).

$$\beta_0 = \gamma_0 + \gamma_1 weekday + \gamma_2 (hour * month) + \gamma_3 holidays + \gamma_4 Tadj, avg_D + \gamma_5 (daylightHours * month) \quad (2)$$

We use hourly weather data to calculate the $Tadj,avg_D$, the average daily temperature adjusted for wind chill index (WCI) and temperature humidity index (THI) (Equations (3) to (6)). For each region, we use data for either Reagan National Airport (DCA) or Pittsburgh International Airport (PIT) (NOAA 2014a), depending on which is closest (Table 2).

Because the relationship between temperature and load is highly nonlinear (Figure 2), we used a nonlinear, additive term to account for temperature in the regression. We found that using a non-linear model of temperature was more accurate than using linear relationships (see Appendix A). The remaining regression terms are linear.

Table 2. Weather station used for each zone's regression

Region	Weather station used
PJM Classic	DCA
Rockland Energy	DCA
Allegheny Energy	DCA
Exelon – Commonwealth Edison	PIT
AEP	PIT
Dayton Power & Light	PIT

Duquesne Light Co	PIT
Dominion Virginia	DCA

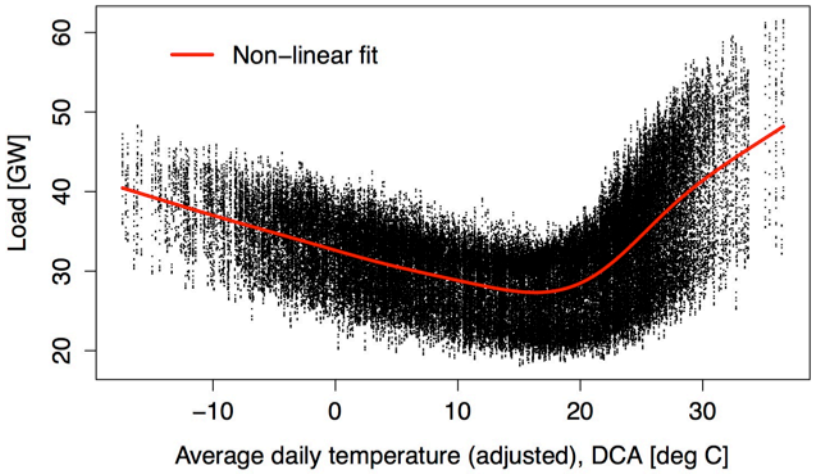

Figure 2. Relationship between hourly load in PJM Classic and adjusted average daily temperature at Reagan National Airport (DCA), 2005 - 2009. Because the relationship is highly nonlinear, we use a non-linear, additive model to account for temperature dependence.

Table 3: Temperature calculations

$$THI_i = c_1 + c_2T_i + c_3R_i + c_4T_iR_i + c_5T_i^2 + c_6R_i^2 + c_7T_i^2R_i + c_8T_iR_i^2 + c_9T_i^2R_i^2 \quad (3)$$

c_1 = -42.379
c_2 = 2.04091523
c_3 = 10.14333127
c_4 = -0.22475541
c_5 = -6.83783×10^{-3}
c_6 = -5.481717×10^{-2}
c_7 = 1.22874×10^{-3}
c_8 = 8.5282×10^{-4}
c_9 = -1.99×10^{-6}

$$WCI_i = 35.74 + 0.6215T_i - 35.75V_i^{0.16} + 0.4275TV_i^{0.16} \quad (4)$$

$$Tadj_i = \begin{cases} THI_i, & \text{if } T_i \geq 80\ ^oF \text{ and } R_i \geq 40\% \\ WCI_i, & \text{if } T_i \leq 50\ ^oF \text{ and } V_i \geq 3 \text{ mph} \\ T_i, & \text{otherwise} \end{cases} \quad (5)$$

$$Tadj,avg_D = mean(Tadj_i), \quad \forall i \in D \quad (6)$$

i = hour of the day
D = day of the year
T_i = hourly temperature [^{o}F]
R_i = hourly relative humidity [percentage value between 0 and 100]
V_i = hourly wind speed [mph]
THI_i = temperature humidity index [^{o}F]
WCI_i = wind chill index [^{o}F]
$Tadj_i$ = hourly adjusted temperature
$Tadj,avg_D$ = daily average adjusted temperature [^{o}F]

WCI index equation from (NOAA 2013); THI index equation based on (NOAA 2014b). Although conversion equations are in English units, the remainder of our analysis uses Celsius.

Step 3: Bootstrap residuals of the stationary model

To account for uncertainty in the underlying process/model, we bootstrap the residuals of the stationary time series model, *Y*, Eq. (2). We bootstrap residuals by month, in 24-hour blocks. Bootstrapping by month allows us to account for heteroskedasticity in the residuals (Figure A.6);

using 24-hour blocks allows us to account for time dependence in the residuals (Figure A.7). The resulting bootstrapped residuals are used in Step 7.

Step 4: Forecast temperatures

Because the next year's temperatures are uncertain, we develop temperature forecasts for 2010 based on historic NOAA weather data dating back to 1949 for DCA and PIT airports (NOAA 2014a) (years 1966 – 1972 were excluded due to missing data). We use hourly temperature, relative humidity, and wind speed data to calculate the average adjusted daily temperature ($Tadj,avg_D$) for DCA and PIT each day (Equations (3) to (6)). We bootstrap days from this 60 year dataset, by month, in 10-day blocks. Bootstrapping by month allows us to account for the seasonal variations in temperature; using 10-day blocks allows us to account for time dependence in weather patterns that can last for several days (Figure A.8) Using 60 years of temperature data allows us to robustly account for extreme temperatures that may occur. We do not observe a secular trend in the NOAA temperature data. By using historic data, we do not account for the possibility of future climate-induced changes in temperature levels or volatility.

Step 5: Forecast the stationary time series

Once we have a model of the underlying stationary process (step 2), we use the model to predict the next year's stationary time series. This stationary time series excludes the effects of load growth. In this prediction, we use the temperature forecast developed in step 4.

Step 6: Forecast load growth

Our forecast of growth in average load is based on PJM's 2009 forecast for 2010 load growth. We adjust the forecast to account for the historic accuracy of the Energy Information Agency's (EIA) load forecasts in the Annual Energy Outlook; insufficient data on PJM forecast accuracy is publically available. Between 1999 – 2008, EIA load growth forecasts had an average bias of -0.3%

and standard deviation of 1.9% (EIA 2008). We assume forecast errors are normally distributed, and develop a distribution of possible load growth rates (Figure 3). We then sample growth rates from the resulting distribution. We assume load growth is linear throughout the year.

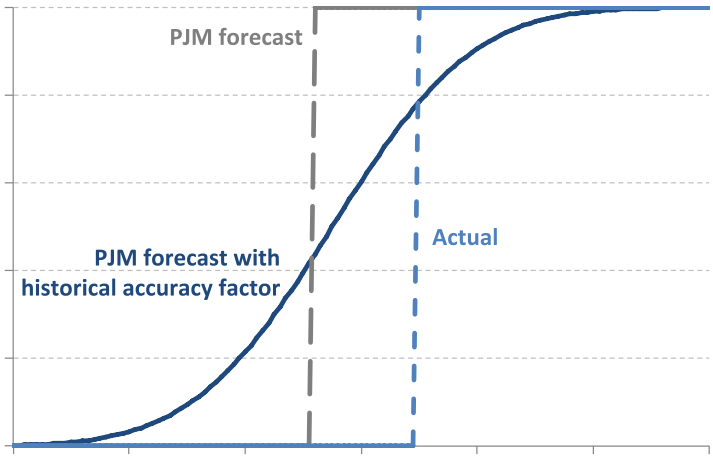

Figure 3. PJM's 2010 load growth forecast, with and without the historical accuracy factor, and actual load growth that occurred.

Step 7: Forecast hourly load

Finally, we sum the three components of our load forecast model: forecast load growth (step 6), the forecast stationary time series (step 5), and the residuals of the stationary time series regression (step 3). This allows us to separately account for the three sources of uncertainty: uncertain load growth, natural temperature variability, and uncertainty in the underlying model/process. As all three components are probabilistic, we repeat the process many times to measure the uncertainty associated with each. The result is a probabilistic hourly forecast of load.

Once we have developed probabilistic hourly load forecasts for each zone, we sum these forecasts to find the total load forecast for PJM. We repeat the entire process 5,000 times to develop a probabilistic forecast of hourly PJM load in 2010.

1.2.2 Supply forecast

We next forecast the total capacity available at each hour. Total available capacity is the summed capacity of all online dispatchable plants, demand response, import capacity, and firm wind capacity. We use data from the 2010 PJM Form EIA-411 to identify each dispatchable plant's summer and winter capacity, as cleared in the capacity auction (PJM 2010b). We therefore assume the system operator has perfect information as to what generators will be available for the forecast year. We simulate the online status of each PJM generator, taking into consideration forced outages, planned outages, and maintenance outages. We simulate total capacity available for each of the 8760 hours of the year, and repeat the simulation 5,000 times to get a distribution of capacity available at each hour. We do not model other supply-side actions PJM can take to mitigate outage risks, such as voltage reductions.

We first schedule planned outages and maintenance outages for all plants. These outages are scheduled such that the likelihood of a supply shortage is minimized. As such, the majority of outages are scheduled during the spring and fall. NERC's Generating Availability Data System (GADS) provides data on the average number of planned outage hours and maintenance outage hours for plants, aggregated by plant type and size (NERC 2014). We find that these outages can be scheduled with minimal effect on LOLE. We schedule each plant's planned outages and maintenance outages with the following process:

1. Find the total planned outage hours (POH) and forced outage hours (FOH) for each plant
2. Divide plants into two categories: peaking plants (<100 MW) and non-peaking plants
3. Schedule peaking outages such that the total offline capacity is roughly equal for all hours of the year. Each plant is assumed to undergo one outage, of duration POH + FOH. ~1.7 GW of peaking capacity is scheduled offline each hour.

4. Schedule non-peaking outages to occur during the spring (March, April, May) and fall (September, October, November). Each plant is assumed to undergo one outage, of duration POH + FOH. ~35 GW of non-peaking capacity is scheduled offline each spring and fall hour.

By scheduling outages in this manner, we minimize the likelihood of a supply shortage. We also mimic the actual scheduling of outages in PJM, in which baseload coal and combined cycle plants are primarily offline during the spring and fall, and combustion turbines are offline throughout the year (Figure A.1).

We next model forced outages. Forced outages are caused by unforeseen technical problems, occur randomly throughout the year, and have an uncertain duration. We model plant forced outages as a two-stage discrete Markov chain (Billinton et al 1973). Figure 4 illustrates this process. At each time period t, if the plant is online there is probability $P_{1,1}$ that it remains on at period t+1 and probability $P_{1,0}$ that is fails. If the plant is offline, it remains off with probability $P_{0,0}$ and is repaired with probability $P_{0,1}$. Accounting for the duration of outages increases the uncertainty of how much capacity is available at each hour. We simulate each plant's forced outages over one year (8760 hours), then sum the total online capacity of all PJM plants. We assume that each plant's transition probabilities are constant throughout the year.

GADS provides data on the mean number of forced outages, and PJM provides data on plant equivalent demand forced outage rates (EFORd) (PJM 2014b). We use these data to calculate the transition probabilities with equations (7) through (11). EFORd is defined as "the probability that a generating unit will fail, either partially or totally, to perform when it is needed to operate" (PJM 2011a). All data are aggregated by plant type and size.

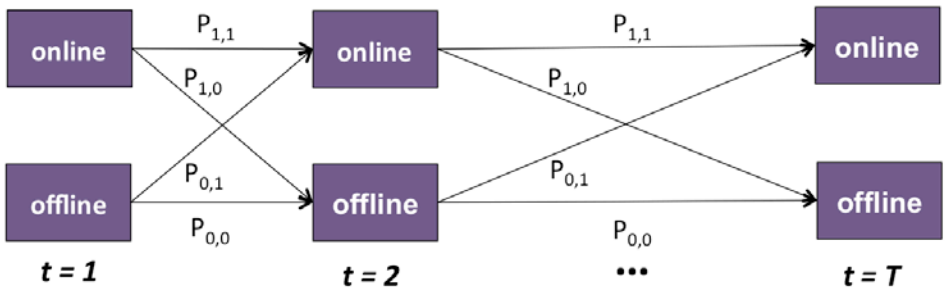

Figure 4. Forced outages 2-stage discrete Markov process

Table 4. Forced outage equations

$$MOD = \frac{EFORd * 8760}{NFO} \quad (7)$$

$$P_{0,1} = \frac{1}{MOD} \quad (8)$$

$$P_{0,0} = 1 - P_{0,1} \quad (9)$$

$$P_{1,0} = \frac{NFO}{8760} \quad (10)$$

$$P_{1,1} = 1 - P_{1,0} \quad (11)$$

MOD = mean outage duration
NFO = Annual number of forced outages
$EFORd$ = Equivalent forced outage rate

We estimate the available DR capacity and net import capacity based on the results of the capacity auctions (PJM 2009) (Table 5). Each auction covers the period of June 1 of the first year to May 31 of the second year. We derate DR capacity by 5%, as is PJM's practice to account for DR that does not respond to PJM requests (PJM 2010a). Firm wind capacity is assumed by PJM to be 13% of nameplate capacity (PJM 2009); for both 2009 and 2010, firm wind capacity was 40 MW.

Table 5. DR capacity and net import capacity, by capacity auction (PJM 2009)

Capacity auction	DR capacity (MW)	Net import capacity (MW)
2009/2010	7,290	+320
2010/2011	9,050	-400

1.2.3 Outage forecast

We assume here that an outage occurs when total load exceeds total available capacity. Using the procedures outlined above, we develop yearly forecasts of hourly load and available capacity. We then subtract the hourly load forecast from the hourly forecast of available capacity to identify if an outage has occurred, Eq. (12). We calculate UE and LOLH with equations (13) and (14) to find the number of outages per ten simulated years. LOLE is calculated in a similar manner as LOLH, but all consecutive outage hours are counted as one outage event. We repeat the process 10,000 times to develop distributions of LOLE, UE, and LOLH. We repeat the entire process, varying the amount of installed capacity in order to see how reliability metrics change versus reserve margin. To vary capacity, we add or subtract a constant amount from each hour's available capacity.

Table 6. Outage equations

$$Outage_i = \begin{cases} 1 : \sum AvailableCapacity_i < Load_i \\ 0 : \sum AvailableCapacity_i > Load_i \end{cases} \quad \forall i \in I \tag{12}$$

$$LOLH = \sum_i Outage_i \quad \forall i \in I \tag{13}$$

$$EUE = \sum_i (Load_i - AvailableCapacity_i) \quad \forall i \in Outage_i = 1 \tag{14}$$

I = set of 8760 annual hours

$AvailableCapacity_i$ = summed capacity of all online PJM generators, DR, net imports, and reliable wind power at hour i

$Load_i$ = total PJM load at hour i

$Outage_i$ = binary variable indicating if an outage occurred at hour i

Our modeling does not consider the effect of transmission constraints on resource adequacy. In the 2009/2010 auction, PJM found inflows were constrained to the Eastern Mid-Atlantic Area Council (EMAAC) and southwestern MAAC. Additional capacity was procured in these regions, resulting in higher capacity prices in these regions (PJM 2008). In the 2010/2011 auction, PJM found no transmission constraints, and capacity prices were equal throughout the interconnection. We also ignore any operating or synchronous reserve requirements.

PJM's Base Residual Auction is held in May, three years prior to the delivery year. By conducting the auction three years in advance, PJM seeks to reduce uncertainty for market participants. Each year after the Base Residual Auction, PJM conducts Incremental Auctions to account for changes in market conditions. Our analysis simulates the last Incremental Auction, one year in advance of the delivery date. As such, we use data from 2009 and earlier to develop the 2010 forecast. In principle, our methods could be used to simulate the Base Residual Auction, but would need to be adjusted to account for the increased uncertainty in available capacity and load three years in advance.

1.2.4 Correlated outages

As one example of correlated outages, we test how LOLE, LOLH, and UE would vary if all 30 GW of PJM natural gas combustion turbines (NGCTs) were subject to the risk of a natural gas supply disruption during winter months (December – February). We model the hourly risk of a fuel supply shortage as $P_{FS.}$ We then evaluate each winter hour if a supply shortage occurs with Eq. (15). We assume the risk of a supply shortage is uniform throughout the winter. If a supply shortage occurs, the probability of each individual NGCT failing is $P_{outage,FS}$, Eq. (16); if no supply shortage occurs, we adjust the probability of an independent failure occurring such that the overall risk of

failure is equal to the case in which all outages are independent, Eq. (10). We therefore do not change the probability of an outage occurring. Rather, we adjust the fraction of outages due to a supply shortage versus an independent failure.

Because data on the frequency and severity of correlated outages is not publically available, we test the sensitivity to each parameter. First, we vary the hourly probability of a supply shortage from 0.093% to 0.008% (twice per winter to once every 5.5 winters), assuming that all NGCTs fail if a shortage occurs ($P_{outage,FS}$ = 1). In the second test, we vary fraction of generators forced offline by a supply shortage from 0% to 100%, assuming that shortage occur on average once per winter (P_{FS} = 0.046%).

Table 7. Correlated outage equations

$$fuelShortage_i = \begin{cases} 1 : rand() \le P_{FS} \\ 0 : rand() > P_{FS} \end{cases} \quad \forall i \in I_{winter} \tag{15}$$

$$P_{1,0,i}' = \begin{cases} P_{outage,FS} : fuelShortage_i = 1 \\ P_{1,0} - P_{outage,FS} * P_{FS} : fuelShortage_i = 0 \end{cases} \quad \forall i \in I_{annual} \tag{16}$$

$$P_{1,1}' = 1 - P_{1,0}' \tag{17}$$

I_{annual} = set of all 8760 annual hours

I_{winter} = set of 2160 winter hours

P_{FS} = Probability of a fuel shortage

$fuelShortage_i$ = binary variable indicating if there is a fuel shortage at hour i

$P_{outage,FS}$ = Probability that a generator goes offline if a fuel shortage occurs

1.3 Results

Table 8 shows accuracy statistics of the load model, both in the training data for 2005-2009 and test data when predicting 2010 load. The test error is the model's prediction error when given actual

2010 temperatures and load growth; it therefore ignores uncertainty in temperature and load growth. Normalized root-mean-square error (NRMSE) controls for the size of the PJM region, Eq. (18). Table A.1 shows detailed regression results for the "PJM Classic" region. Figure 5 shows training and test residuals distributions. Because the distributions are similar, resampling from the training residuals should reasonably account for model uncertainty (see Methods - Step 3).

$$NRMSE = \frac{RMSE}{load_{max} - load_{min}} \tag{18}$$

Table 8. Accuracy statistics of the load forecast model, both training error (1993 – 2009) and test prediction error (2010).

	Training, 1993 - 2009		Test, 2010	
PJM Region	**RMSE [MW]**	**NRMSE [%]**	**RMSE [MW]**	**NRMSE [%]**
PJM Classic	1690	4.0	1800	4.5
AEP	790	5.2	910	6.7
Allegheny Energy	300	5.3	330	6.2
Dayton Power & Light	130	4.7	140	6.1
Dominion Virginia	640	3.3	760	5.8
Duquesne Light Co	80	4.1	90	5.2
Exelon – Commonwealth Edison	930	5.6	1000	6.9
Rockland Energy	20	4.2	20	5.1
PJM total	3510	3.5	3840	4.3

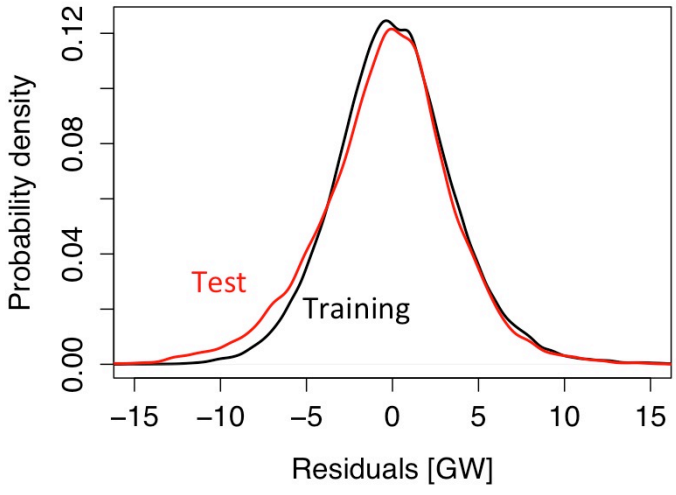

Figure 5. Distribution of training residuals and test residuals for PJM total.

The model's accuracy could certainly be improved further. Including weather data from more points within PJM would likely have the greatest effect on model accuracy. Our model uses weather data from Reagan National and Pittsburgh International Airports; PJM's long-term load forecasting model uses temperature data from 24 airports (PJM 2013).

1.3.1 The effect of temperature and load growth uncertainty

Our probabilistic forecast of 2010 load considers uncertainty in temperature, load growth, and model error. Figure 6 illustrates the model's accuracy when these uncertain factors are considered. Although the actual load is within the forecast's 95% confidence bounds, the forecast is biased to somewhat under-predict the probability of high loads. This is because 2010 had an unusually high number of days with temperatures between 20 ºC and 25 ºC (Figure 7). Using actual 2010 temperatures and load growth instead of probabilistic forecasts removes the model's bias to underpredict the probability of high loads (Figure 6).

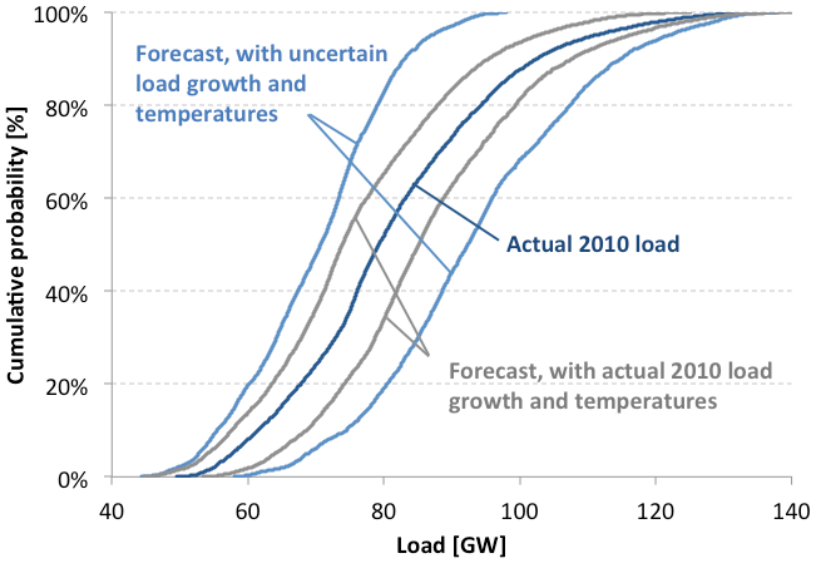

Figure 6. Accuracy of load model. Cumulative probability of actual 2010 hourly load, and forecasts' 95% confidence intervals.

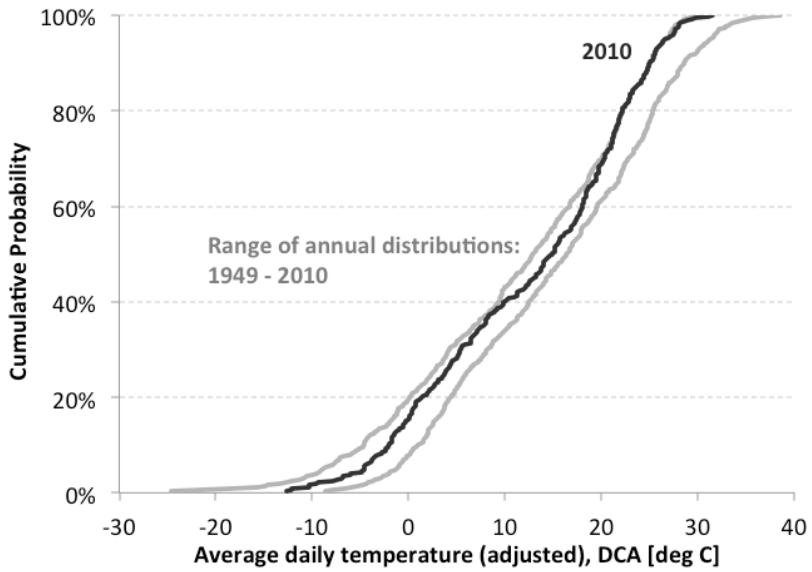

Figure 7. 2010 temperature distributions, and 95% confidence interval of temperature distributions from 1949 – 2010. 2010 had an unusually high number of days with average adjusted temperatures of 20 °C – 25 °C.

1.3.2 Reliability metrics

Figure 8 shows simulated 2010 LOLE for reserve margins of 10% to 25%. The expected value of our 2010 simulation closely matches that of PJM's 2013 simulation (data on PJM's 2010 simulation is not available, but the results of the simulation have changed very little over time). In 2010, PJM found a 15.5% reserve margin was necessary to meet the 0.1 LOLE standard (PJM 2010a); we find a 15.5% reserve margin would have resulted in an LOLE of 0.09 events per year. Our simulation's 90% confidence interval ranges from zero to three events per ten years at 15.5% reserve margin.

The actual 2010 reserve margin was 20.5% (164 GW), as PJM procured more capacity than was needed on the capacity market (PJM 2008)[2]. We find that a 20.5% reserve margin corresponds to an expected LOLE of 0.02 events per year, and achieves the 0.1 LOLE standard with 90% confidence.

[2] Generation offered + fixed resource requirement (FRR) commitments – generation offered but not accepted

Therefore, PJM's revealed risk preference in 2010 was to meet the 0.1 LOLE standard with 90% confidence.

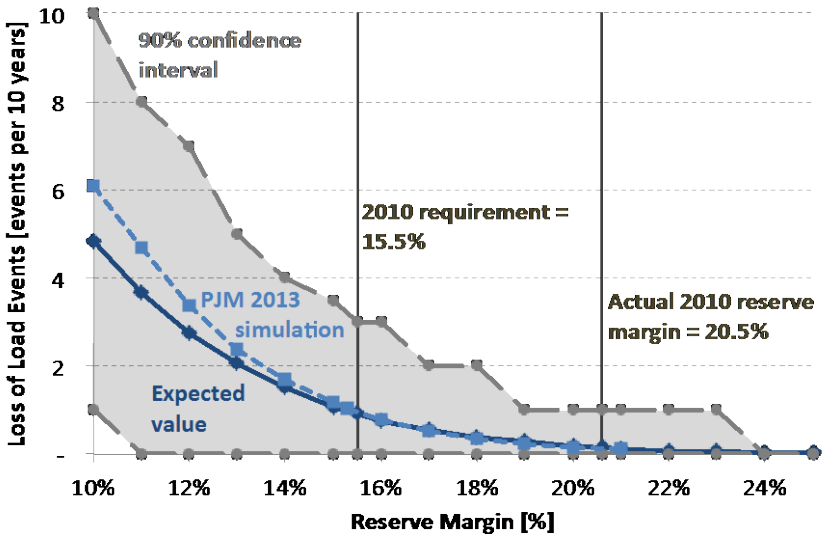

Figure 8. 2010 LOLE versus reserve margin. Also shown are results from PJM's 2013 resource adequacy modeling (recreated from (PJM 2010a)).

Figure 9 shows simulated 2010 unserved energy versus reserve margin. At a 15.5% reserve margin, the expected UE is 1.5 GWh per year, or 0.0002% of actual 2010 load. The 90% confidence interval ranges from 0 GWh per year to 7.5 GWh per year (0.0000% - 0.0011% of load unserved, respectively). UE becomes increasingly uncertain at lower reserve margins. Expected LOLH is 4, with a 90% confidence range of 0 to 16.

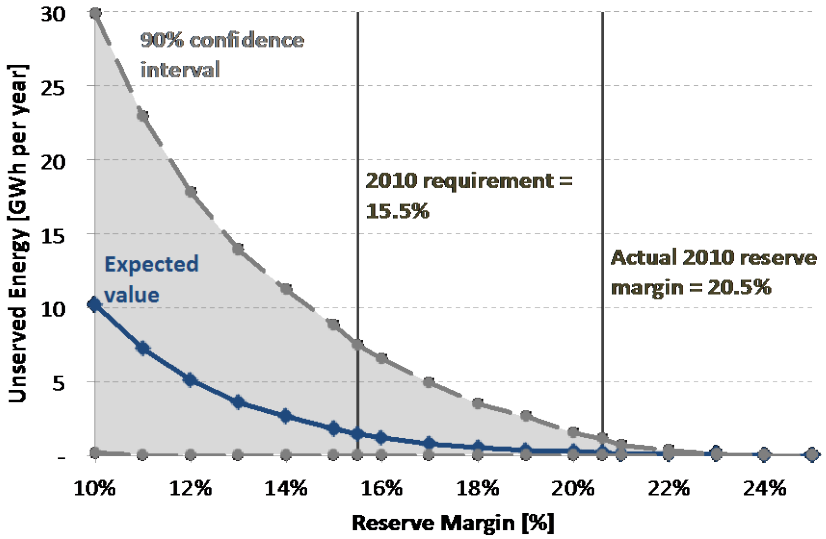

Figure 9. 2010 unserved energy versus reserve margin.

1.3.3 Optimal reserve margin and the effects of risk aversion

We find that PJM's target 2010 reserve margin of 15.5% was sufficient to meet the 0.1 LOLE standard. Switching to either the 2.4 LOLH standard or the 0.001% UE standard could reduce reserve margins to 10% or 11% (Table 9). By procuring additional capacity such that the realized reserve margin was 20.5%, PJM's implied risk preference is to meet the 0.1 LOLE standard with 90% confidence. PJM could meet the 2.4 LOLH standard and 0.001% UE standard with 90% confidence at reserve margins of 13% and 14%, respectively. Requiring that the reliability metric be met with 95% or 99% confidence would further increase reserve margin requirements.

Table 9. Sensitivity of the target reserve margin and installed capacity to different reliability metrics and risk tolerances. PJM's target 2010 reserve margin was 15.5% (158 GW), and actual 2010 reserve margin was 20.5% (165 GW).

	Optimal reserve margin [%] (installed capacity [GW])			
Metric	**Risk Neutral**	**90% Confidence**	**95% Confidence**	**99% Confidence**
0.1 LOLE	15.5% (158)	20.5% (165)	23% (168)	>25% (>170)

2.4 LOLH	10% (151)	13% (154)	14% (156)	16% (159)
0.001% UE	11% (152)	14% (156)	16% (159)	18% (161)

1.3.4 Distribution of outage size

We find that there is extreme variation in the amount of load shed during outages. As shown in Figure 10, the distribution of unserved energy resulting from an outage is extremely fat tailed. At a 15.5% reserve margin, the mean outage is 15 GWh, but outages range from 0 GWh to 126 GWh (Table 10). The top 10% largest outages account for half of total unserved energy, and the top 1% of outages account for 10% of total unserved energy. The risk of a very large outage becomes more pronounced at lower reserve margins.

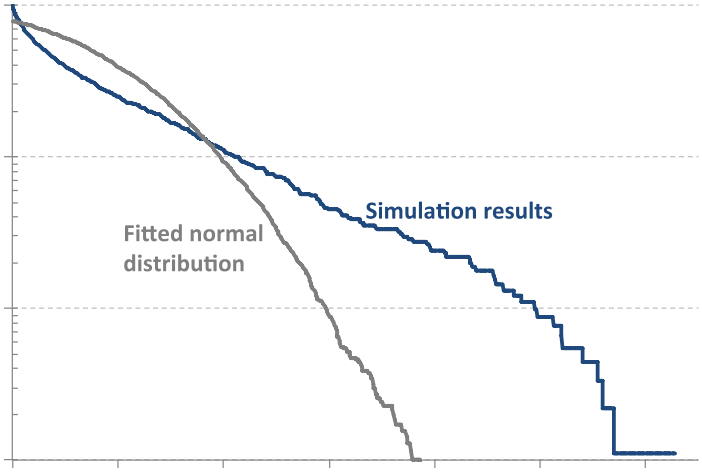

Figure 10. Distribution of the size of simulated outages, in terms of unserved energy, versus a fitted normal distribution. Assumed reserve margin is 15.5%.

Table 10. Outage summary statistics, 15.5% reserve margin

	Expected value	90% Confidence Interval	Maximum
Outage duration [hours]	4	1 - 9	11

Largest magnitude [GW]	4	0 - 11	18
Total load shed [GWh]	15	0 - 58	126

1.3.5 Model form uncertainty

Load in PJM is highly sensitive to temperature, and accurately modeling this relationship is important for accurately calculating LOLE. We used a nonparametric, additive model to account for the relationship between load and temperature. We also tested a linear model to account for the relationship. The linear model divided days into heating degree days (HDD) and cooling degree days (CDD). Details can be found in Appendix A. We find that the linear model significantly over-predicts load at high temperature hours, which increases the modeled probability of outages relative to the nonparametric, additive model (Figure 11).

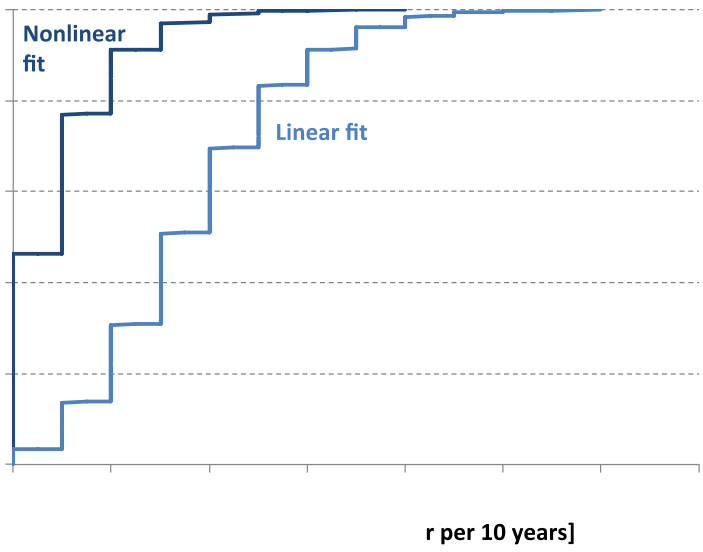

Figure 11. Comparison of LOLE estimates for non-parametric and linear temperature models at 15.5% reserve margin. The linear model overestimates load at high temperature hours, and therefore overestimates the probability of an outage occurring.

We also analyze the sensitivity of the model's parameters to 'leave-one-out' testing (Figure 12). The base model uses data from 2005 – 2009 to estimate model parameters. Estimating model parameters from only four years' worth of data, leaving one of the years out, would change model

parameters and therefore estimates of LOLE, LOLH, and UE. The baseline expected value of LOLE is 0.9 at a 15.5% reserve margin; 'leave-one-out' testing can vary the mean LOLE by +/- 30% (0.64 to 0.97).

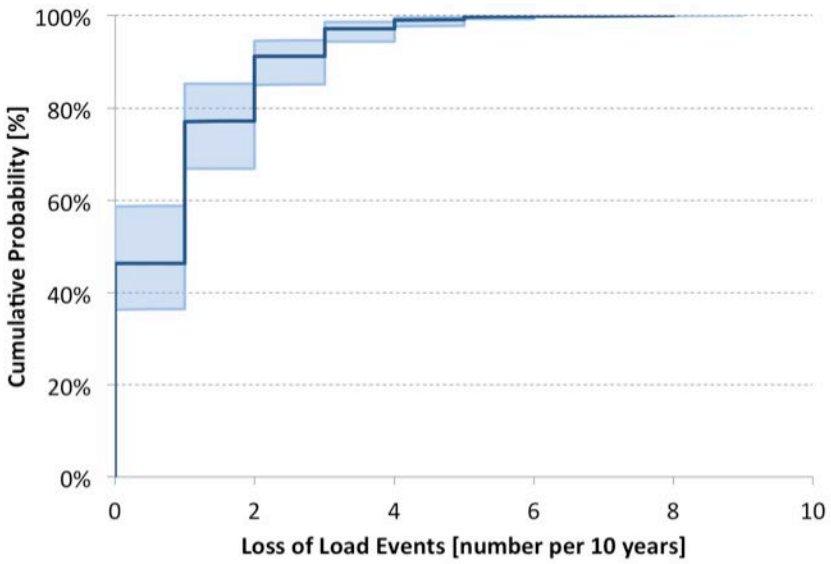

Figure 12. Sensitivity of LOLE to 'leave-one-out' parameter testing. The base model (solid line) estimates parameters with data from 2005 – 2009. The shaded area shows the range of results if one year's worth of data is left out when estimating the parameters. Evaluated at 15.5% reserve margin.

Finally, we test the sensitivity of results to a scenario in which EFORd varies with ambient temperature. We find that LOLE would increase if EFORd rose in summer months and fell in winter months. For more details, see Appendix A.

1.3.6 Correlated failures

We find that natural gas supply disruptions during the winter have the potential to increase the risk of a supply shortage, assuming such outages force a large percentage of PJM's NGCTs offline at once. If a supply disruption that forces all 30 GW of NGCTs offline occurs on average once every year, the expected UE increases by 40%.

The risk posed by supply disruptions increases significantly if outages are not constrained to only occur during winter months. If unconstrained supply disruptions that force all 30 GW of NGCT capacity offline were to occur on average once every five years, expected UE would double (Figure 13). If unconstrained supply disruptions were to occur on average once per year, expected UE would increase by more than 10 times. However, supply disruptions pose a significant risk only if they force more than 50% of NGCTs offline at once (Figure A.10). Supply disruptions can significantly increase the maximum size of supply shortages (Figure A.11).

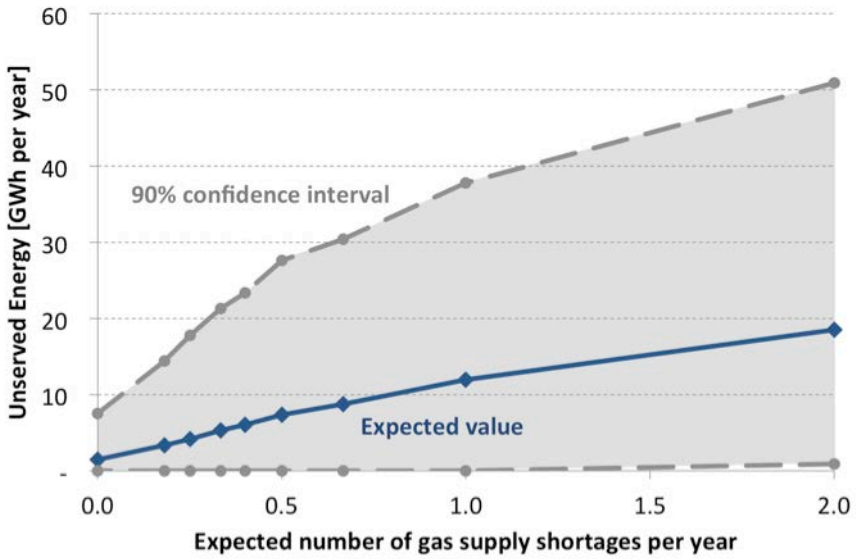

Figure 13. Sensitivity of unserved energy to natural gas supply shortages that can occur at any point during the year, and force all PJM NGCTs offline. Evaluated at 15.5% IRM.

1.4 Discussion

Using our probabilistic regression method, we find the 2010 reserve margin target of 15.5% was sufficient to meet the mandated 0.1 LOLE standard. PJM procured 7 GW more capacity than needed to meet the 15.5% target, making the realized reserve margin 20.5%. By procuring more capacity than needed, PJM's revealed 2010 risk preference was to meet the 0.1 LOLE standard with 90% confidence. This risk aversion is due to PJM's policy to procure more capacity than needed if

the capacity can be procured at a cost less than the net cost of new entry of a natural gas combustion turbine (~$270/MW-day) (PJM 2008, Spees et al 2011).

Switching from the 0.1 LOLE standard to either the 2.4 LOLH or 0.001% UE standard would have reduced PJM's 20.5% reserve margin in 2010. A 14% reserve margin would have been sufficient to meet the 0.001% UE standard with 90% confidence. A 13% reserve margin would have been sufficient to meet the 2.4 LOLH standard with 90% confidence. This represents a 9 GW – 11 GW reduction in capacity procurement, while still maintaining levels of reliability accepted by other systems. If PJM were to switch to either standard, the 11 GW of coal capacity "at high risk" of retirement could be retired without needing to be replaced.

NERC recommends that PJM adopt a reliability metric based on unserved energy. We agree. The LOLE metric is flawed, in that it measures only the probability of an outage occurring and ignores both the severity and duration of outages. Our modeling shows that the severity and duration of outage events vary greatly (Table 10), undermining the usefulness of the LOLE metric. Because supply shortages could cause political fallout both regionally and for PJM management, we recommend that PJM work through their stakeholder process to identify both the appropriate UE target and the risk tolerance of PJM participants.

System operators should be aware that the risk posed by supply shortages is primarily due to extremely severe, but infrequent outages. Our simulations show that the largest 10% of supply shortages are responsible for 50% of unserved energy. Taking into account the possibility of correlated generator outages further exacerbates this risk. The risk of very large outages increases at low reserve margins, suggesting that some risk aversion on part of PJM may be justified. System operators should work to ensure that their system is robust to large supply shortages, and that these shortages do not lead to cascading network failures.

PJM's resource adequacy modeling assumes that generator outages are independent. We find that correlated outages among plants due to natural gas supply shortages could increase outage risk, and cause PJM to underestimate this risk. Evidence suggests that correlated outages do occur with some regularity; winter storms on January 7, 2013 led to 19 GW of natural gas plants and 21 GW of other capacity simultaneously experiencing forced outages (PJM 2014c). We recommend further research into the risks posed by correlated outages. If the risks posed by correlated outages are found to be significant, we recommend that PJM consider this risk when planning resource adequacy needs. If correlated outage risks are found to be significant, PJM may need to significantly increase reserve margins.

1.5 Acknowledgements

The authors acknowledge support from the Doris Duke Charitable Foundation, the Richard King Mellon Foundation, The Heinz Endowments, and the Carnegie Mellon Electricity Industry Center. This research was also supported in part by the Climate and Energy Decision Making (CEDM) center, created through a cooperative agreement between the National Science Foundation (SES-0949710) and Carnegie Mellon University. This research was also supported by the U.S. Department of Energy's National Energy Technology Laboratory. The authors thank Kathleen Spees for helpful discussions.

Appendix A

Scheduling planned outages and maintenance outages

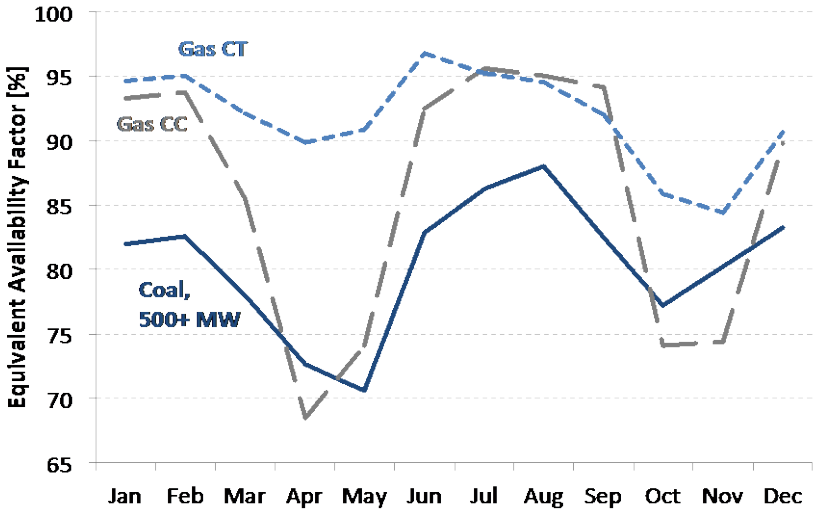

Figure A.1. Equivalent availability factor, PJM generators, 2010 (Bresler, 2012).

Detailed Regression Results

Table A.1 provides detailed regression results for the PJM Classic region. We find that the significant results have the expected sign in most cases. For example, signs are negative for holidays, reflecting that load are lower on these days. Signs are also negative for low-load hours during the night and positive for high-load hours during the day and evening.

Table A.1. Detailed regression results for the PJM Classic region.

Note: Dependent variable is residuals from the long-term trend regression (see main paper, step 1).
*Significance codes: '***' (P < 0.001); '**' (P < 0.01); '*' (P < 0.05); '.' (P < 0.1); ' ' (P < 1)*

Variable	Estimate	Std. Error	t value	Significance	Notes
(Intercept)	1.81E-01	2.82E-02	6.42	***	
isTue	1.06E-02	6.83E-04	15.551	***	

Variable	Estimate	Std. Error	t value	Significance	Notes
isWed	1.39E-02	6.84E-04	20.32	***	
isThu	1.46E-02	6.87E-04	21.199	***	
isFri	1.67E-03	6.92E-04	2.417	*	
isSat	-8.53E-02	6.86E-04	-124.412	***	
isSun	-1.15E-01	6.87E-04	-167.982	***	
isMLK	-1.07E-02	3.53E-03	-3.036	**	
isPresidentsDay	3.24E-03	3.55E-03	0.913		
isGoodFriday	-5.23E-02	3.50E-03	-14.933	***	
isMemorialDay	-1.01E-01	4.28E-03	-23.616	***	
isMemorialDayWeekend	-2.92E-02	2.73E-03	-10.701	***	
isJuly4	-1.14E-01	3.57E-03	-31.912	***	
isLaborDay	-1.13E-01	4.26E-03	-26.464	***	
isLaborDayWeekend	-2.25E-02	2.63E-03	-8.572	***	
isChristmas	-1.41E-01	4.65E-03	-30.313	***	
isXmasEveEve	-1.56E-03	4.65E-03	-0.335		Dec 23
isChristmasEve	-7.55E-02	4.65E-03	-16.234	***	Dec 24
isXMasWk	-2.49E-02	3.51E-03	-7.091	***	Dec 26 - 30
XMasLights	1.39E-02	2.65E-03	5.256	***	Dec 4 - Dec 22
isThanksgiving	-1.50E-01	3.80E-03	-39.4	***	
isThanksgivingFriday	-1.01E-01	3.80E-03	-26.556	***	Day after Thanksgiving
isNewYearsDay	-9.74E-02	3.62E-03	-26.935	***	
isNewYearsEve	-5.05E-02	4.55E-03	-11.086	***	
isThanksgivingWeek	-4.39E-03	1.95E-03	-2.249	*	Mon - Sun, Thanksgiving week
isXmasDayAfter	-4.66E-02	3.84E-03	-12.129	***	Dec 26
isFeb	5.69E-01	3.58E-02	15.918	***	
isH1	-1.27E-01	3.18E-03	-40.034	***	
isH2	-1.58E-01	3.18E-03	-49.564	***	
isH3	-1.71E-01	3.18E-03	-53.732	***	
isH4	-1.72E-01	3.18E-03	-53.952	***	
isH5	-1.52E-01	3.18E-03	-47.793	***	
isH6	-9.37E-02	3.18E-03	-29.479	***	
isH7	1.63E-04	3.18E-03	0.051		
isH8	5.40E-02	3.18E-03	16.975	***	
isH9	6.73E-02	3.18E-03	21.169	***	
isH10	7.31E-02	3.18E-03	23.001	***	
isH11	7.34E-02	3.18E-03	23.104	***	
isH12	6.48E-02	3.18E-03	20.401	***	
isH13	5.12E-02	3.18E-03	16.099	***	
isH14	3.93E-02	3.18E-03	12.356	***	
isH15	2.67E-02	3.18E-03	8.407	***	
isH16	2.58E-02	3.18E-03	8.13	***	

Variable	Estimate	Std. Error	t value	Significance	Notes
isH17	5.70E-02	3.18E-03	17.928	***	
isH18	1.31E-01	3.18E-03	41.196	***	
isH19	1.45E-01	3.18E-03	45.666	***	
isH20	1.32E-01	3.18E-03	41.475	***	
isH21	1.11E-01	3.18E-03	34.75	***	
isH22	6.89E-02	3.18E-03	21.672	***	
isH23	3.30E-03	3.18E-03	1.039		
isH24	-6.95E-02	3.18E-03	-21.878	***	
isMar	7.45E-01	3.44E-02	21.642	***	
isApr	6.17E-01	3.65E-02	16.902	***	
isMay	1.35E-02	4.38E-02	0.309		
isJun	-2.49E+00	1.18E-01	-21.184	***	
isJul	1.13E+00	6.13E-02	18.502	***	
isAug	1.88E-02	3.87E-02	0.486		
isSep	1.85E-02	3.64E-02	0.51		
isOct	3.60E-01	3.41E-02	10.542	***	
isNov	5.39E-01	3.87E-02	13.929	***	
isDec	1.57E+00	1.08E-01	14.539	***	
sun.hours	6.30E-04	4.99E-05	12.617	***	Daily daylight length, DC [mins]
isFeb:isH1	2.94E-02	4.54E-03	6.474	***	
isFeb:isH2	3.16E-02	4.54E-03	6.966	***	
isFeb:isH3	3.40E-02	4.54E-03	7.483	***	
isFeb:isH4	3.58E-02	4.54E-03	7.88	***	
isFeb:isH5	3.75E-02	4.54E-03	8.259	***	
isFeb:isH6	4.06E-02	4.54E-03	8.939	***	
isFeb:isH7	4.15E-02	4.54E-03	9.139	***	
isFeb:isH8	3.38E-02	4.54E-03	7.456	***	
isFeb:isH9	3.47E-02	4.54E-03	7.645	***	
isFeb:isH10	3.13E-02	4.54E-03	6.888	***	
isFeb:isH11	2.77E-02	4.54E-03	6.106	***	
isFeb:isH12	2.42E-02	4.54E-03	5.324	***	
isFeb:isH13	2.12E-02	4.54E-03	4.675	***	
isFeb:isH14	1.90E-02	4.54E-03	4.179	***	
isFeb:isH15	1.67E-02	4.54E-03	3.678	***	
isFeb:isH16	1.22E-02	4.54E-03	2.695	**	
isFeb:isH17	-1.80E-03	4.54E-03	-0.396		
isFeb:isH18	-2.08E-02	4.54E-03	-4.584	***	
isFeb:isH19	1.29E-02	4.54E-03	2.848	**	
isFeb:isH20	1.84E-02	4.54E-03	4.051	***	
isFeb:isH21	2.00E-02	4.54E-03	4.403	***	
isFeb:isH22	2.13E-02	4.54E-03	4.693	***	

Variable	Estimate	Std. Error	t value	Significance	Notes
isFeb:isH23	2.30E-02	4.54E-03	5.076	***	
isFeb:isH24	2.53E-02	4.54E-03	5.569	***	
isH1:isMar	2.86E-02	4.42E-03	6.465	***	
isH2:isMar	2.71E-02	4.42E-03	6.126	***	
isH3:isMar	2.66E-02	4.43E-03	6.004	***	
isH4:isMar	2.71E-02	4.42E-03	6.143	***	
isH5:isMar	2.91E-02	4.42E-03	6.59	***	
isH6:isMar	3.70E-02	4.42E-03	8.378	***	
isH7:isMar	3.87E-02	4.42E-03	8.766	***	
isH8:isMar	4.10E-02	4.42E-03	9.294	***	
isH9:isMar	4.69E-02	4.42E-03	10.619	***	
isH10:isMar	4.77E-02	4.42E-03	10.795	***	
isH11:isMar	4.78E-02	4.42E-03	10.816	***	
isH12:isMar	4.71E-02	4.42E-03	10.674	***	
isH13:isMar	4.68E-02	4.42E-03	10.593	***	
isH14:isMar	4.64E-02	4.42E-03	10.498	***	
isH15:isMar	4.38E-02	4.42E-03	9.908	***	
isH16:isMar	3.60E-02	4.42E-03	8.163	***	
isH17:isMar	1.15E-02	4.42E-03	2.605	**	
isH18:isMar	-3.91E-02	4.42E-03	-8.847	***	
isH19:isMar	-4.31E-03	4.42E-03	-0.977		
isH20:isMar	2.86E-02	4.42E-03	6.465	***	
isH21:isMar	3.68E-02	4.42E-03	8.326	***	
isH22:isMar	3.57E-02	4.42E-03	8.073	***	
isH23:isMar	3.13E-02	4.42E-03	7.093	***	
isH24:isMar	2.67E-02	4.42E-03	6.045	***	
isH1:isApr	1.16E-02	4.48E-03	2.599	**	
isH2:isApr	-8.57E-04	4.48E-03	-0.191		
isH3:isApr	-1.03E-02	4.51E-03	-2.291	*	
isH4:isApr	-1.44E-02	4.48E-03	-3.209	**	
isH5:isApr	-1.68E-02	4.48E-03	-3.74	***	
isH6:isApr	-9.50E-03	4.48E-03	-2.122	*	
isH7:isApr	-4.69E-03	4.48E-03	-1.048		
isH8:isApr	9.13E-03	4.48E-03	2.039	*	
isH9:isApr	3.21E-02	4.48E-03	7.178	***	
isH10:isApr	4.73E-02	4.48E-03	10.555	***	
isH11:isApr	5.98E-02	4.48E-03	13.365	***	
isH12:isApr	6.93E-02	4.48E-03	15.469	***	
isH13:isApr	7.69E-02	4.48E-03	17.172	***	
isH14:isApr	8.28E-02	4.48E-03	18.502	***	
isH15:isApr	8.44E-02	4.48E-03	18.859	***	

Variable	Estimate	Std. Error	t value	Significance	Notes
isH16:isApr	7.70E-02	4.48E-03	17.194	***	
isH17:isApr	4.43E-02	4.48E-03	9.89	***	
isH18:isApr	-2.95E-02	4.48E-03	-6.597	***	
isH19:isApr	-4.54E-02	4.48E-03	-10.138	***	
isH20:isApr	-1.11E-02	4.48E-03	-2.486	*	
isH21:isApr	4.66E-02	4.48E-03	10.399	***	
isH22:isApr	5.28E-02	4.48E-03	11.788	***	
isH23:isApr	4.11E-02	4.48E-03	9.186	***	
isH24:isApr	2.47E-02	4.48E-03	5.521	***	
isH1:isMay	-2.65E-02	4.56E-03	-5.812	***	
isH2:isMay	-4.77E-02	4.56E-03	-10.455	***	
isH3:isMay	-6.37E-02	4.56E-03	-13.978	***	
isH4:isMay	-7.67E-02	4.56E-03	-16.82	***	
isH5:isMay	-8.53E-02	4.56E-03	-18.709	***	
isH6:isMay	-8.81E-02	4.56E-03	-19.331	***	
isH7:isMay	-9.21E-02	4.56E-03	-20.197	***	
isH8:isMay	-6.09E-02	4.56E-03	-13.356	***	
isH9:isMay	-2.11E-02	4.56E-03	-4.626	***	
isH10:isMay	1.01E-02	4.56E-03	2.223	*	
isH11:isMay	3.71E-02	4.56E-03	8.13	***	
isH12:isMay	5.92E-02	4.56E-03	12.994	***	
isH13:isMay	7.75E-02	4.56E-03	17.009	***	
isH14:isMay	9.32E-02	4.56E-03	20.442	***	
isH15:isMay	1.04E-01	4.56E-03	22.723	***	
isH16:isMay	1.03E-01	4.56E-03	22.628	***	
isH17:isMay	7.35E-02	4.56E-03	16.118	***	
isH18:isMay	-4.76E-03	4.56E-03	-1.045		
isH19:isMay	-3.53E-02	4.56E-03	-7.745	***	
isH20:isMay	-3.06E-02	4.56E-03	-6.721	***	
isH21:isMay	1.95E-02	4.56E-03	4.27	***	
isH22:isMay	4.21E-02	4.56E-03	9.243	***	
isH23:isMay	2.59E-02	4.56E-03	5.685	***	
isH24:isMay	1.37E-03	4.56E-03	0.3		
isH1:isJun	-1.33E-01	6.46E-03	-20.594	***	
isH2:isJun	-1.63E-01	6.46E-03	-25.214	***	
isH3:isJun	-1.88E-01	6.46E-03	-29.167	***	
isH4:isJun	-2.10E-01	6.46E-03	-32.541	***	
isH5:isJun	-2.28E-01	6.46E-03	-35.239	***	
isH6:isJun	-2.49E-01	6.46E-03	-38.536	***	
isH7:isJun	-2.67E-01	6.46E-03	-41.394	***	
isH8:isJun	-2.28E-01	6.46E-03	-35.286	***	

Variable	Estimate	Std. Error	t value	Significance	Notes
isH9:isJun	-1.68E-01	6.46E-03	-26.041	***	
isH10:isJun	-1.18E-01	6.46E-03	-18.229	***	
isH11:isJun	-7.30E-02	6.46E-03	-11.307	***	
isH12:isJun	-3.42E-02	6.46E-03	-5.288	***	
isH13:isJun	-1.52E-03	6.46E-03	-0.234		
isH14:isJun	2.60E-02	6.46E-03	4.024	***	
isH15:isJun	4.75E-02	6.46E-03	7.355	***	
isH16:isJun	5.42E-02	6.46E-03	8.385	***	
isH17:isJun	2.65E-02	6.46E-03	4.101	***	
isH18:isJun	-5.42E-02	6.46E-03	-8.397	***	
isH19:isJun	-9.27E-02	6.46E-03	-14.353	***	
isH20:isJun	-1.07E-01	6.46E-03	-16.592	***	
isH21:isJun	-9.39E-02	6.46E-03	-14.533	***	
isH22:isJun	-6.30E-02	6.46E-03	-9.746	***	
isH23:isJun	-7.39E-02	6.46E-03	-11.446	***	
isH24:isJun	-9.86E-02	6.46E-03	-15.263	***	
isH1:isJul	3.13E-02	4.90E-03	6.4	***	
isH2:isJul	-9.19E-04	4.90E-03	-0.188		
isH3:isJul	-2.99E-02	4.90E-03	-6.107	***	
isH4:isJul	-5.57E-02	4.90E-03	-11.372	***	
isH5:isJul	-7.88E-02	4.90E-03	-16.098	***	
isH6:isJul	-1.07E-01	4.90E-03	-21.945	***	
isH7:isJul	-1.48E-01	4.90E-03	-30.185	***	
isH8:isJul	-1.16E-01	4.90E-03	-23.785	***	
isH9:isJul	-4.95E-02	4.90E-03	-10.106	***	
isH10:isJul	1.15E-02	4.90E-03	2.349	*	
isH11:isJul	6.66E-02	4.90E-03	13.598	***	
isH12:isJul	1.15E-01	4.90E-03	23.4	***	
isH13:isJul	1.55E-01	4.90E-03	31.573	***	
isH14:isJul	1.87E-01	4.90E-03	38.222	***	
isH15:isJul	2.12E-01	4.90E-03	43.326	***	
isH16:isJul	2.21E-01	4.90E-03	45.119	***	
isH17:isJul	1.94E-01	4.90E-03	39.662	***	
isH18:isJul	1.14E-01	4.90E-03	23.296	***	
isH19:isJul	7.45E-02	4.90E-03	15.213	***	
isH20:isJul	5.32E-02	4.90E-03	10.871	***	
isH21:isJul	5.90E-02	4.90E-03	12.056	***	
isH22:isJul	8.59E-02	4.90E-03	17.552	***	
isH23:isJul	7.95E-02	4.90E-03	16.23	***	
isH24:isJul	6.15E-02	4.90E-03	12.557	***	
isH1:isAug	-1.60E-02	4.48E-03	-3.57	***	

Variable	Estimate	Std. Error	t value	Significance	Notes
isH2:isAug	-4.49E-02	4.48E-03	-10.022	***	
isH3:isAug	-7.22E-02	4.48E-03	-16.118	***	
isH4:isAug	-9.64E-02	4.48E-03	-21.53	***	
isH5:isAug	-1.18E-01	4.48E-03	-26.299	***	
isH6:isAug	-1.39E-01	4.48E-03	-31.018	***	
isH7:isAug	-1.74E-01	4.48E-03	-38.891	***	
isH8:isAug	-1.57E-01	4.48E-03	-35.129	***	
isH9:isAug	-9.56E-02	4.48E-03	-21.352	***	
isH10:isAug	-3.69E-02	4.48E-03	-8.232	***	
isH11:isAug	1.73E-02	4.48E-03	3.853	***	
isH12:isAug	6.52E-02	4.48E-03	14.567	***	
isH13:isAug	1.05E-01	4.48E-03	23.494	***	
isH14:isAug	1.38E-01	4.48E-03	30.847	***	
isH15:isAug	1.63E-01	4.48E-03	36.395	***	
isH16:isAug	1.71E-01	4.48E-03	38.156	***	
isH17:isAug	1.43E-01	4.48E-03	31.836	***	
isH18:isAug	6.06E-02	4.48E-03	13.53	***	
isH19:isAug	1.92E-02	4.48E-03	4.299	***	
isH20:isAug	4.13E-03	4.48E-03	0.922		
isH21:isAug	2.70E-02	4.48E-03	6.029	***	
isH22:isAug	3.24E-02	4.48E-03	7.246	***	
isH23:isAug	2.01E-02	4.48E-03	4.48	***	
isH24:isAug	3.15E-03	4.48E-03	0.704		
isH1:isSep	-2.96E-02	4.48E-03	-6.603	***	
isH2:isSep	-5.28E-02	4.48E-03	-11.8	***	
isH3:isSep	-7.29E-02	4.48E-03	-16.288	***	
isH4:isSep	-9.00E-02	4.48E-03	-20.102	***	
isH5:isSep	-1.04E-01	4.48E-03	-23.172	***	
isH6:isSep	-1.09E-01	4.48E-03	-24.309	***	
isH7:isSep	-1.06E-01	4.48E-03	-23.76	***	
isH8:isSep	-1.00E-01	4.48E-03	-22.41	***	
isH9:isSep	-5.75E-02	4.48E-03	-12.845	***	
isH10:isSep	-1.41E-02	4.48E-03	-3.152	**	
isH11:isSep	2.48E-02	4.48E-03	5.534	***	
isH12:isSep	5.79E-02	4.48E-03	12.928	***	
isH13:isSep	8.69E-02	4.48E-03	19.415	***	
isH14:isSep	1.12E-01	4.48E-03	25.011	***	
isH15:isSep	1.31E-01	4.48E-03	29.165	***	
isH16:isSep	1.35E-01	4.48E-03	30.26	***	
isH17:isSep	1.07E-01	4.48E-03	23.929	***	
isH18:isSep	2.63E-02	4.48E-03	5.865	***	

Variable	Estimate	Std. Error	t value	Significance	Notes
isH19:isSep	-5.96E-03	4.48E-03	-1.332		
isH20:isSep	2.19E-02	4.48E-03	4.892	***	
isH21:isSep	3.78E-02	4.48E-03	8.452	***	
isH22:isSep	2.63E-02	4.48E-03	5.871	***	
isH23:isSep	7.17E-03	4.48E-03	1.603		
isH24:isSep	-1.35E-02	4.48E-03	-3.014	**	
isH1:isOct	-1.58E-02	4.41E-03	-3.572	***	
isH2:isOct	-3.00E-02	4.39E-03	-6.834	***	
isH3:isOct	-4.09E-02	4.41E-03	-9.264	***	
isH4:isOct	-4.90E-02	4.41E-03	-11.094	***	
isH5:isOct	-5.28E-02	4.41E-03	-11.971	***	
isH6:isOct	-4.45E-02	4.41E-03	-10.078	***	
isH7:isOct	-2.13E-02	4.41E-03	-4.818	***	
isH8:isOct	-7.60E-03	4.41E-03	-1.723	.	
isH9:isOct	1.05E-02	4.41E-03	2.39	*	
isH10:isOct	2.83E-02	4.41E-03	6.42	***	
isH11:isOct	4.42E-02	4.41E-03	10.024	***	
isH12:isOct	5.70E-02	4.41E-03	12.915	***	
isH13:isOct	6.85E-02	4.41E-03	15.525	***	
isH14:isOct	7.82E-02	4.41E-03	17.723	***	
isH15:isOct	8.39E-02	4.41E-03	19.011	***	
isH16:isOct	8.04E-02	4.41E-03	18.219	***	
isH17:isOct	5.33E-02	4.41E-03	12.073	***	
isH18:isOct	-9.01E-03	4.41E-03	-2.043	*	
isH19:isOct	6.71E-03	4.41E-03	1.522		
isH20:isOct	3.96E-02	4.41E-03	8.976	***	
isH21:isOct	3.67E-02	4.41E-03	8.307	***	
isH22:isOct	2.87E-02	4.41E-03	6.505	***	
isH23:isOct	1.46E-02	4.41E-03	3.311	***	
isH24:isOct	-7.66E-05	4.41E-03	-0.017		
isH1:isNov	2.41E-03	4.51E-03	0.535		
isH2:isNov	-4.85E-03	4.50E-03	-1.076		
isH3:isNov	-9.05E-03	4.51E-03	-2.008	*	
isH4:isNov	-1.14E-02	4.51E-03	-2.529	*	
isH5:isNov	-9.98E-03	4.51E-03	-2.214	*	
isH6:isNov	-1.68E-03	4.51E-03	-0.372		
isH7:isNov	5.75E-03	4.51E-03	1.274		
isH8:isNov	6.81E-03	4.51E-03	1.511		
isH9:isNov	2.07E-02	4.51E-03	4.589	***	
isH10:isNov	2.84E-02	4.51E-03	6.288	***	
isH11:isNov	3.27E-02	4.51E-03	7.243	***	

Variable	Estimate	Std. Error	t value	Significance	Notes
isH12:isNov	3.67E-02	4.51E-03	8.132	***	
isH13:isNov	4.00E-02	4.51E-03	8.865	***	
isH14:isNov	4.29E-02	4.51E-03	9.508	***	
isH15:isNov	4.50E-02	4.51E-03	9.968	***	
isH16:isNov	4.59E-02	4.51E-03	10.186	***	
isH17:isNov	5.32E-02	4.51E-03	11.807	***	
isH18:isNov	5.24E-02	4.51E-03	11.63	***	
isH19:isNov	3.94E-02	4.51E-03	8.739	***	
isH20:isNov	3.54E-02	4.51E-03	7.86	***	
isH21:isNov	3.14E-02	4.51E-03	6.966	***	
isH22:isNov	2.61E-02	4.51E-03	5.798	***	
isH23:isNov	1.94E-02	4.51E-03	4.306	***	
isH24:isNov	1.15E-02	4.51E-03	2.553	*	
isH1:isDec	6.61E-02	6.13E-03	10.793	***	
isH2:isDec	5.80E-02	6.13E-03	9.457	***	
isH3:isDec	5.33E-02	6.13E-03	8.701	***	
isH4:isDec	5.13E-02	6.13E-03	8.377	***	
isH5:isDec	5.10E-02	6.13E-03	8.319	***	
isH6:isDec	5.08E-02	6.13E-03	8.289	***	
isH7:isDec	4.80E-02	6.13E-03	7.832	***	
isH8:isDec	4.83E-02	6.13E-03	7.879	***	
isH9:isDec	5.57E-02	6.13E-03	9.082	***	
isH10:isDec	5.85E-02	6.13E-03	9.54	***	
isH11:isDec	5.69E-02	6.13E-03	9.284	***	
isH12:isDec	5.56E-02	6.13E-03	9.073	***	
isH13:isDec	5.51E-02	6.13E-03	8.985	***	
isH14:isDec	5.54E-02	6.13E-03	9.048	***	
isH15:isDec	5.78E-02	6.13E-03	9.44	***	
isH16:isDec	6.27E-02	6.13E-03	10.231	***	
isH17:isDec	8.43E-02	6.13E-03	13.749	***	
isH18:isDec	9.31E-02	6.13E-03	15.199	***	
isH19:isDec	8.20E-02	6.13E-03	13.376	***	
isH20:isDec	8.16E-02	6.13E-03	13.31	***	
isH21:isDec	8.43E-02	6.13E-03	13.757	***	
isH22:isDec	8.79E-02	6.13E-03	14.35	***	
isH23:isDec	8.79E-02	6.13E-03	14.34	***	
isH24:isDec	7.92E-02	6.13E-03	12.922	***	
isFeb:sun.hours	-9.88E-04	6.12E-05	-16.132	***	
isMar:sun.hours	-1.26E-03	5.78E-05	-21.739	***	
isApr:sun.hours	-1.08E-03	5.87E-05	-18.32	***	
isMay:sun.hours	-3.03E-04	6.47E-05	-4.684	***	

Variable	Estimate	Std. Error	t value	Significance	Notes
isJun:sun.hours	2.66E-03	1.43E-04	18.647	***	
isJul:sun.hours	-1.58E-03	8.15E-05	-19.384	***	
isAug:sun.hours	-2.29E-04	6.01E-05	-3.82	***	
isSep:sun.hours	-2.20E-04	5.93E-05	-3.715	***	
isOct:sun.hours	-7.31E-04	5.81E-05	-12.582	***	
isNov:sun.hours	-1.02E-03	6.72E-05	-15.176	***	
isDec:sun.hours	-2.85E-03	1.93E-04	-14.738	***	

Linear model results

We use a non-parametric, additive model to account for the relationship between adjusted average daily temperature and hourly load (see Methods - Step 2). However, we also investigated the potential of using a linear model to account for the relationship. As discussed below, we found that using a linear fit worked well for the majority of hours, but considerably over-predicted loads during high temperature days. This over prediction led to the linear model over-estimating the probability of a supply shortage.

The linear model we used in the second step considered the maximum and minimum daily temperature, as shown in Eq. (A.1). We divided days into heating degree days (HDD) and cooling degree days (CDD), as is common in literature (A.2). The split temperature between HDD/CDD was set to minimize model error: for Tmax terms, the temperature was 20.6 °C. For Tmin terms, temperature was 7.2 °C. We then used a linear and quadratic term for both HDD and CDD temperatures in the regression (A.3).

Table A.2. Temperature calculations

$$Tmax_D = max\ Tadj_i, \quad \forall i \in D$$
$$Tmin_D = min\ Tadj_i \quad \forall i \in D \qquad \text{(A.1)}$$

$$Tmax.HDD = max(69 - Tmax_D, 0)$$
$$Tmax.CDD = max(Tmax_D - 69, 0) \qquad \text{(A.2)}$$

$Tmin.HDD = max(45 - Tmin_D, 0)$
$Tmin.CDD = max(Tmin_D - 45, 0)$

i = hour of the day
D = day of the year
$Tadj_i$ = hourly adjusted temperature
$Tmax_D$, $Tmin_D$ = daily max and min temperature [°F]

$$\beta_0 = \gamma_0 + \gamma_1 weekday + \gamma_2 (hour*month) + \gamma_3 holidays + \gamma_4 Tmax.HDD + \gamma_5 Tmax.CDD + \gamma_6 Tmin.HDD + \gamma_7 Tmin.CDD + \gamma_8 Tmax.HDD^2 + \gamma_9 Tmax.CDD^2 + \gamma_{10} Tmin.HDD^2 + \gamma_{11} Tmin.CDD^2 + \gamma_{12} (daylightHours*month) \quad \text{(A.3)}$$

As shown in Figure A.2 –Figure A.4, the linear model significantly over-predicts load during high-temperature days. This is because the linear model predicts exponential growth in load with increasing temperatures. However, load growth actually begins to slow once a average daily temperatures of ~27 °C are reached (Figure 2). This is likely because air conditioning loads start to saturate once temperatures are high enough. This overprediction of peak load hours causes the linear model to overstate LOLE (Figure A.5). Due to this bias in the linear model, we use a non-linear model in our main analysis.

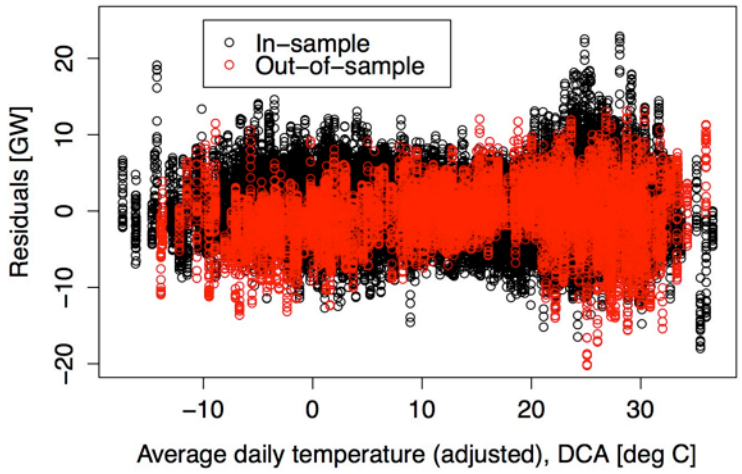

Figure A.2. In-sample and out-of-sample residuals for PJM, linear model. Residuals are large at high temperature days.

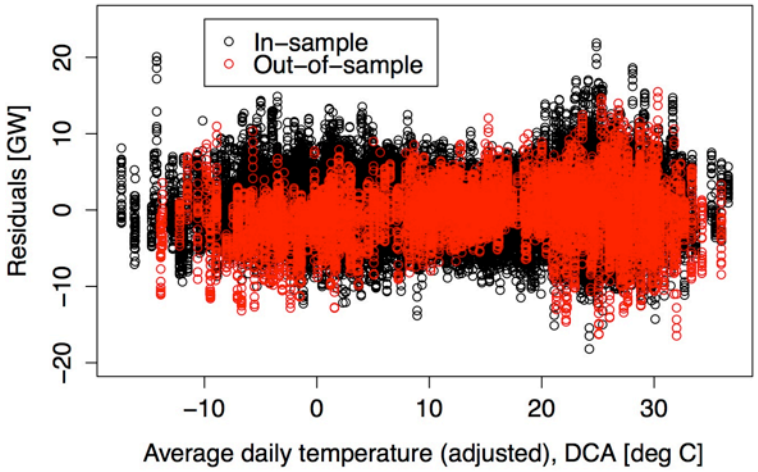

Figure A.3. In-sample and out-of-sample residuals for PJM, non-linear model. The model is more accurate at predicting load during high temperature days than the linear model.

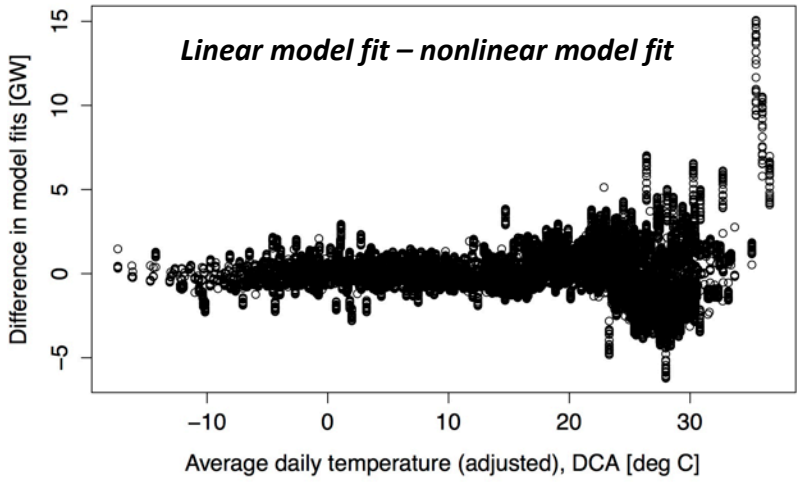

Figure A.4. Difference in linear and nonlinear model fits, when predicting load out-of-sample.

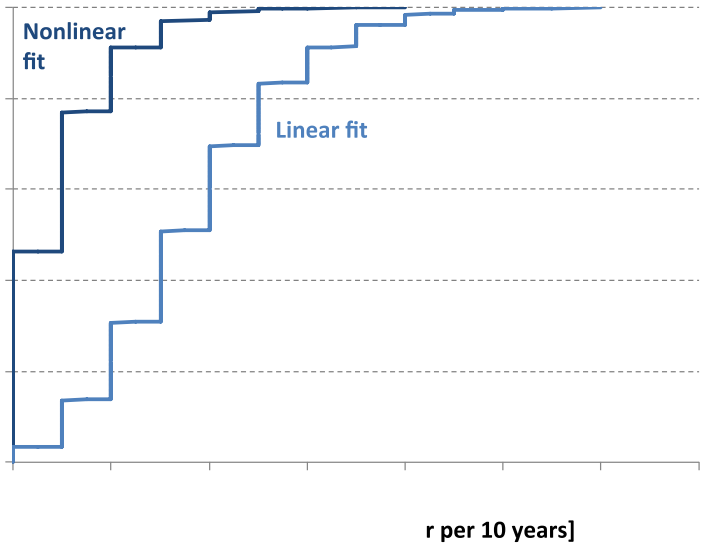

Figure A.5. Calculated LOLE for linear and nonlinear models

Residuals and temperature analysis

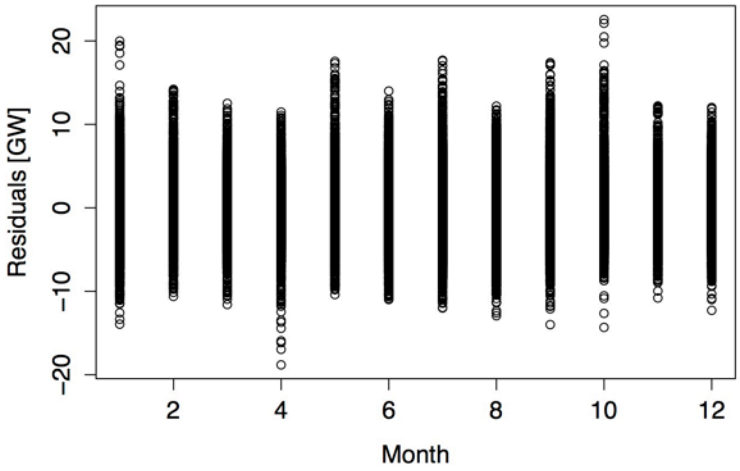

Figure A.6. In-sample residuals, by month

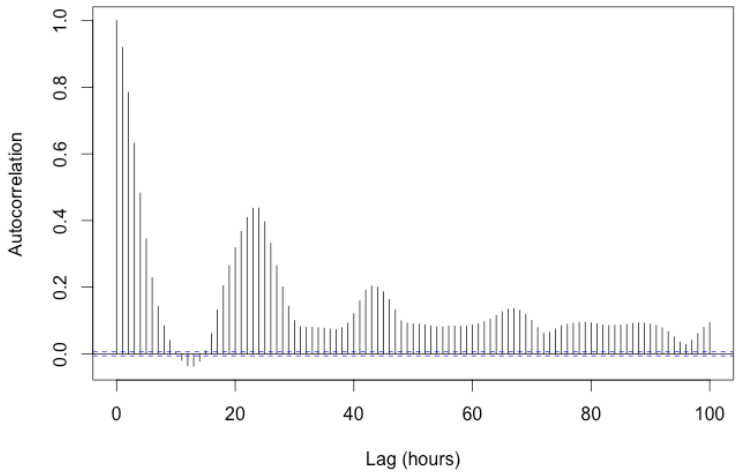

Figure A.7. Autocorrelation of in-sample residuals

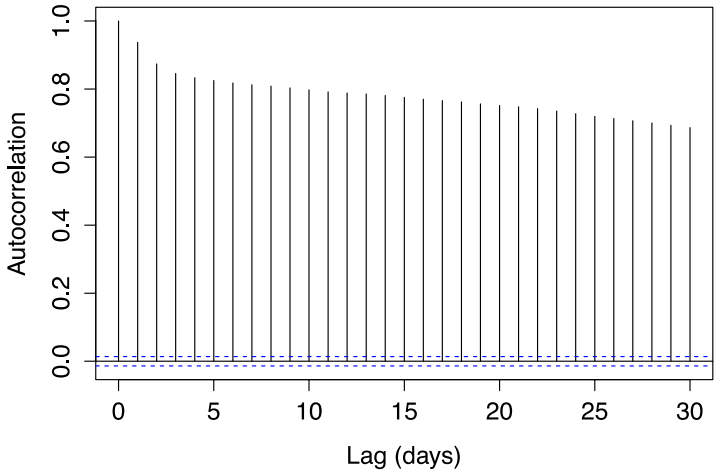

Figure A.8. Autocorrelation function, average adjusted daily temperature. Data is for years 1949 – 2010, except 1966 – 1972.

LOLE sensitivity to forced outage rate

In our regressions, we hold each plant's forced outage rate (EFORd) constant throughout the year. Here we test the effects on LOLE of EFORd being sensitive to ambient temperature, with plants being 50% less likely to be forced offline during the warmest 6 months (April – September)

and 50% more likely to be forced offline in the coolest 6 months (October – March). Figure A.11 shows varying EFORd in this manner more than doubles the expected value of LOLE.

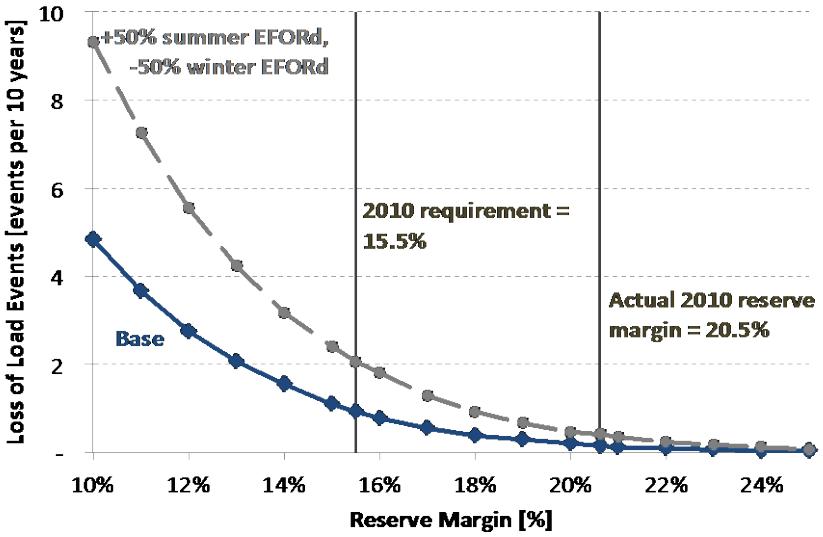

Figure A.9. Sensitivity of LOLE expected value to forced outage rate (EFORd).

Correlated outages

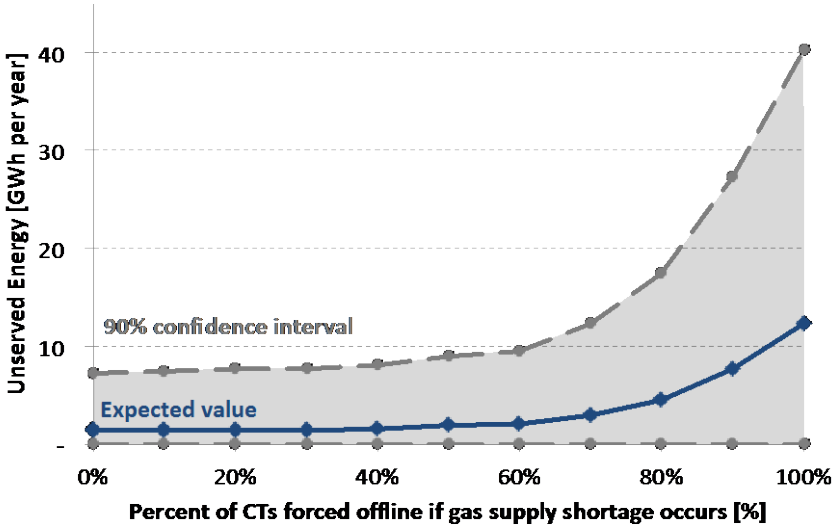

Figure A.10. Sensitivity of unserved energy to natural gas supply shortages that occur on average once per year, at any point during the year (not constrained to winter months). Evaluated at 15.5% IRM.

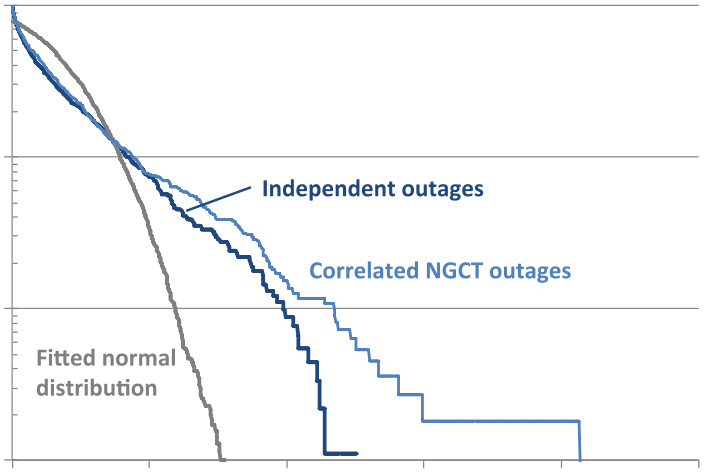

Figure A.11. Distribution of outage size, in terms of unserved energy. Shown are both scenario in which outages are independent, and a scenario in which a natural gas supply shortage occurs on average once per year at any point during the year (not constrained to winter months), forcing 50% of NGCTs offline at once. Assumed reserve margin is 15.5%.

1.6 References

Billington, R., Ringlee, R., Wood, A., 1973. Power-System Reliability Calculations. MIT Press.

Bresler, S., PJM, 2012. Personal communication.

Eastern Interconnection States' Planning Council (EISPC), 2013. The Economic Ramifications of Resource Adequacy White Paper. Available at <http://www.naruc.org/grants/Documents/Economics%20of%20Resource%20Adequacy%20WhitePaper_Astrape_Final.pdf>. (accessed September 2014).

Energy Information Agency (EIA), 2008. Annual Energy Outlook reports, 1999 - 2008. Available at <http://www.eia.gov/forecasts/aeo/archive.cfm>. Accessed August 2014.

Energy Information Agency (EIA), 2014. Annual Energy Outlook 2014 Early Release. Available at: <http://www.eia.gov/forecasts/aeo/er/index.cfm>. (accessed July 2014).

Hagan, M. T., Behr, S. M., 1987. The time series approach to short term load forecasting. Power Systems, IEEE Transactions on, 2(3), 785-791.

Hastie, T, 2013. Package 'gam' documentation. Available at < http://cran.r-project.org/web/packages/gam/gam.pdf>. Accessed January 2015.

Hines, P., Apt, J., Talukdar, S., 2009. Large blackouts in North America: Historical trends and policy implications. Energy Policy, 37(12), 5249-5259.

Hippert, H. S., Pedreira, C. E., & Souza, R. C., 2001. Neural networks for short-term load forecasting: A review and evaluation. *Power Systems, IEEE Transactions on*, *16*(1), 44-55.

Joskow, P., Tirole, J., 2009. Reliability and competitive electricity markets. The Rand Journal of Economics, 38(1), 60-84.

Newell, S. A., Spees, K., Pfeifenberger, J., Karkatsouli, I., 2014. Estimating the Economically Optimal Reserve Margin in ERCOT. Available at <http://brattle.com/system/news/pdfs/000/000/613/original/Estimating_the_Economically_Optimal_Reserve_Margin_in_ERCOT.pdf?1391445083>. Accessed November 2014.

North American Electric Reliability Corporation (NERC), 2010. Final Report on Methodologies and Metrics - September and December, 2010 with Approvals and Revisions. Available at <http://www.nerc.com/comm/PC/Reliability%20Assessment%20Subcommittee%20RAS%20DL/GTRPMTF_Meth__Metrics_Report_final_w%20_PC_approvals_revisions_12%2008%2010.pdf>. (accessed July 2014).

North American Electric Reliability Corporation (NERC), 2014. Generator Availability Data System. Available at <http://www.nerc.com/pa/RAPA/gads/Pages/default.aspx>. Accessed August 2014.

Pfeifenberger, J., Spees, K., Carden, K., Wintermantel, N. (2013). Resource Adequacy Requirements: Reliability and Economic Implications. Available at < https://www.ferc.gov/legal/staff-reports/2014/02-07-14-consultant-report.pdf>. (accessed September 2014).

PJM Interconnection, 2003. PJM Generation Adequacy Analysis: Technical Methods. Available at <http://www.pjm.com/~/media/etools/oasis/references/whitepaper-sections-12.ashx>. (accessed September 2014).

PJM Interconnection, 2008. 2010/2011 RPM Base Residual Auction Results. Available at <http://www.pjm.com/~/media/markets-ops/rpm/rpm-auction-info/20080201-2010-2011-bra-report.ashx>. Accessed July 2014.

PJM Interconnection, 2009. 2012/2013 RPM Base Residual Auction Results. Available at <http://www.pjm.com/~/media/markets-ops/rpm/rpm-auction-info/2012-13-base-residual-auction-report-document-pdf.ashx>. Accessed June 2014.

PJM Interconnection, 2010a. 2010 PJM Reserve Requirement Study. Available at <http://www.pjm.com/~/media/documents/reports/2010-pjm-reserve-requirement-study.ashx>. Accessed July 2014.

PJM Interconnection, 2010b. EIA 411 Report. Available at <http://www.pjm.com/documents/reports/eia-reports.aspx>. Accessed June 2014.

PJM Interconnection, 2011a. 2010 State of the Market Report for PJM, Volume 2. Available at <http://www.monitoringanalytics.com/reports/pjm_state_of_the_market/2010/2010-som-pjm-volume2.pdf>. (accessed September 2014).

PJM Interconnection, 2011b. Coal Capacity at Risk of Retirement in PJM: Potential Impacts of the Finalized EPA Cross State Air Pollution Rule and Proposed National Emissions Standards for Hazardous Air

Pollutants. Available at <http://pjm.com/~/media/documents/reports/20110826-coal-capacity-at-risk-for-retirement.ashx>. (accessed July, 2014)

PJM Interconnection, 2013. PJM Manual 19: Load Forecasting and Analysis, Revision 23. Available at <http://www.pjm.com/~/media/documents/manuals/m19.ashx>. (accessed September 2014).

PJM Interconnection, 2014a. Historical Metered Load Data. Available at <http://www.pjm.com/markets-and-operations/ops-analysis/historical-load-data.aspx>. Accessed June 2014.

PJM Interconnection, 2014b. PJM Monthly EFORd Data. Available at <http://www.pjm.com/markets-and-operations/energy/real-time/historical-bid-data/eford.aspx>. Accessed June 2014.

PJM Interconnection, 2014c. Analysis of Operational Events and Market Impacts During the January 2014 Cold Weather Events. Available at <http://www.pjm.com/~/media/documents/reports/20140509-analysis-of-operational-events-and-market-impacts-during-the-jan-2014-cold-weather-events.ashx>. Accessed November 2014.

Spees, K., Newell, S. A., Carlton, R., Zhou, B., Pfeifenberger, J., 2011. Cost of New Entry Estimates For Combustion Turbine and Combined-Cycle Plants in PJM.

Spees, K., Newell, S., Pfeifenberger, J., 2013. Capacity Markets-Lessons Learned from the First Decade. Economics of Energy & Environmental Policy 2.2.

U.S. National Oceanic and Atmospheric Administration (NOAA), 2013. NWS Windchill Chart. Available at <http://www.nws.noaa.gov/os/windchill/index.shtml>. Accessed August 2014.

U.S. National Oceanic and Atmospheric Administration (NOAA), 2014a. National Climatic Data Center website. Available at

<http://cdo.ncdc.noaa.gov/pls/plclimprod/poemain.accessrouter?datasetabbv=DS3505>. Accessed June 2014.

U.S. National Oceanic and Atmospheric Administration (NOAA), 2014b. NWS Weather Service Heat Index. Available at <http://nws.noaa.gov/os/heat/index.shtml>. Accessed August 2014.

U.S. Naval Observatory, 2012. Duration of Daylight/Darkness Table for One Year. Available at <http://aa.usno.navy.mil/data/docs/Dur_OneYear.php>. Accessed June 2014.